


Optimized synthesis and pharmacological evaluation of HCN channel inhibitor EC18

Marius Patberg¹ | Tengiz Oniani² | Paul Disse³ | Stefan Peischard³ |
 Laura Vinnenberg⁴ | Mehrnough Zobeiri² | Maria N. Romanelli⁵ | Lisa Epping⁴ |
 Heinz Wiendl⁴ | Sven G. Meuth⁶ | Petra Hundehege⁴ | Guiscard Seeböhm³ |
 Thomas Budde² | Anna Junker¹ 

¹European Institute for Molecular Imaging (EIMI), Münster, Germany

²Institut für Physiologie I, Münster, Germany

³Cellular Electrophysiology and Molecular Biology, Institute for Genetics of Heart Diseases (IfGH), University of Münster, Münster, Germany

⁴Klinik für Neurologie mit Institut für Translationale Neurologie, ICB, Münster, Germany

⁵Department of Neurosciences, Psychology, Drug Research and Child Health (NeuroFarBa), University of Florence, Florence, Italy

⁶Universitätsklinikum Düsseldorf, Medizinische Fakultät, Klinik für Neurologie, Düsseldorf, Germany

Correspondence

Anna Junker, European Institute for Molecular Imaging (EIMI), Waldeyerstr. 15, Münster 48149, Germany.
 Email: anna.junker@wwu.de

Funding information

Deutsche Forschungsgemeinschaft, Grant/Award Numbers: BU1019/16-1, GRK2515/1-1, INST 2105/27-1 FUGG, JU 2966/2-1

Abstract

HCN4 channels are considered to be a promising target for cardiac pathologies, epilepsy, and multiple sclerosis. However, there are no subtype-selective HCN channel blockers available, and only a few compounds are reported to display subtype preferences, one of which is EC18 (*cis-1*). Herein, we report the optimized synthetic route for the preparation of EC18 and its evaluation in three different pharmacological models, allowing us to assess its activity on cardiac function, thalamocortical neurons, and immune cells.

KEYWORDS

EC18, HCN4, HCN channel, ion channels, iPSC

1 | INTRODUCTION

The homotetrameric hyperpolarization-activated cyclic nucleotide-gated ion channel 4 (HCN4) plays an essential role in the control of the heart pace in the sinoatrial node^[1] and is highly expressed in the thalamic nuclei,^[2,3] in generating pacemaker activity critical for the generation of slow-wave sleep oscillations.^[4] Altered expression of HCN channels, especially increased levels in thalamic neurons^[5] is associated with the hyper-synchronous neuronal network activity

leading to seizure generalization.^[6] Recently, altered expression of HCN channels has been found in rodents fed with cuprizone-inducing global demyelination in the brain as one important hallmark of multiple sclerosis (MS) pathophysiology.^[7,8] Here, general de- and remyelination are associated with a transient period of neuronal hyperexcitability and increased availability of HCN channels in the thalamus. The systemic administration of ivabradine, a preferential HCN4 channel blocker, is reported to block spontaneous absence seizures.^[9] However, targeting HCN channel-dependent conditions

Marius Patberg and Tengiz Oniani contributed equally to this study.

This is an open access article under the terms of the Creative Commons Attribution-NonCommercial-NoDerivs License, which permits use and distribution in any medium, provided the original work is properly cited, the use is non-commercial and no modifications or adaptations are made.

© 2023 The Authors. *Archiv der Pharmazie* published by Wiley-VCH GmbH on behalf of Deutsche Pharmazeutische Gesellschaft.

in the thalamus may require HCN4-specific modulators. Due to the lack of HCN4-specific inhibitors, EC18 (*cis*-**1**) remains an attractive pharmacological tool, enabling HCN channel-modulation studies with some specificity for HCN4 (EC_{50} [HCN4] = $3.98 \pm 1.16 \mu\text{M}$) over HCN1 (EC_{50} = $21.00 \pm 3.98 \mu\text{M}$) and HCN2 (EC_{50} = $19.35 \pm 4.48 \mu\text{M}$).^[10] HCN channels are considered to be a promising target for cardiac pathologies, epilepsy, and MS. HCN4 channels underly the cardiac pacemaker channel conducting the current I_f in the human sinus node. Recently, we have established iPSC-derived pacemaker cells that closely resemble human sinus node pacemaker cells. These cells generate a rhythmic activity based on HCN4 function similar to the human sinus node, enabling disease modeling and allowing for HCN4 pharmacology in a human pace sinus node-like maker system.^[11] Herein, we present the evaluation of EC18 (*cis*-**1**) in the iPSC-derived pacemaker cell model, in the thalamic neurons, and on T cell activation. Therefore further improving the understanding of its pharmacological characteristics.

2 | RESULTS AND DISCUSSION

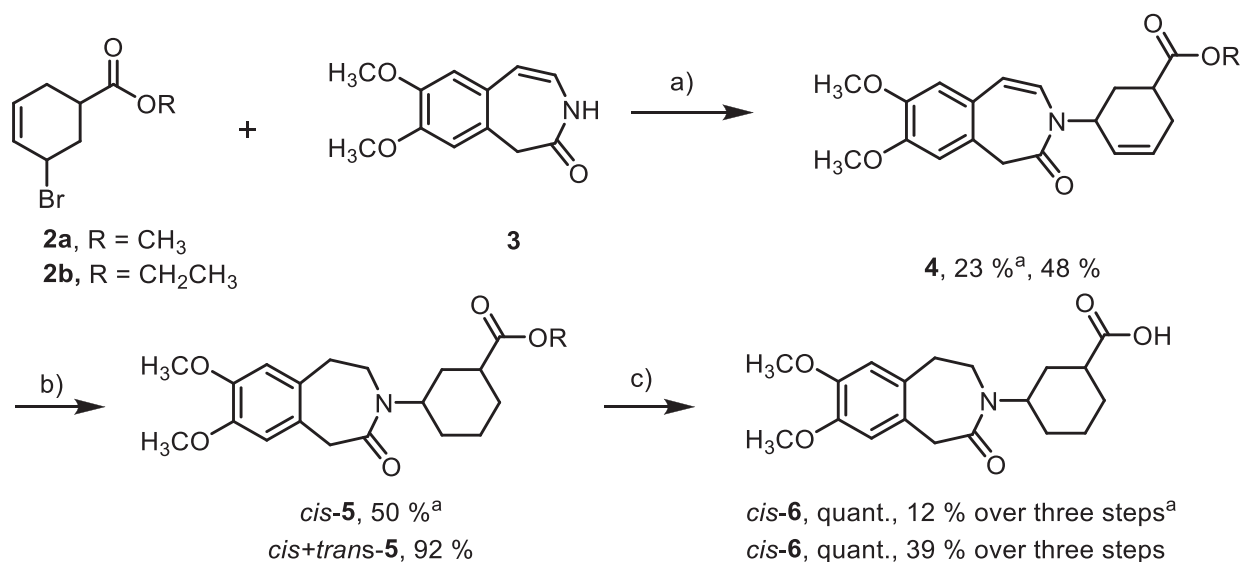
2.1 | Chemistry

As we were interested in further characterization of EC18 in rodent models of absence epilepsy and MS, we required larger quantities of EC18. The main drawback in the synthetic route for the preparation of *cis*-**1** (EC18), initially published by Romanelli et al., is the low overall yield. This is mainly attributable to the synthetic steps leading from building blocks **2** and **3** to the carboxylic acid *cis*-**6**. Linkage of the building blocks forming substituted lactam **4** provided low yields and poor stereoselectivity. Furthermore, chromatographic separation of the *cis*/*trans* isomers was laborious, even if conducted after the

hydrogenation reaction. The purified ester *cis*-**5** was then saponified to yield the acid *cis*-**6** for subsequent Curtius rearrangement (Scheme 1).^[10] We decided to investigate the synthesis of EC18 closer with the aim of improving the overall yield.

The lactam **3** was prepared according to the procedure described by Reiffen et al.^[12] In the synthesis published by Romanelli et al., bromocyclohexene methyl ester **2a** was reacted with lactam **3**.^[10] In the course of this work, we prepared the ethyl ester **2b** instead as we did not expect the ester functionality to have any effect on the stereoselectivity of the reaction.

The reaction of the bromocyclohexene ester **2b** and the lactam **3** under basic conditions led to the formation of compound **4** in 48 % c yield and an 8:2 [*cis*:*trans*]-ratio. As the separation of the *trans* and *cis* esters **4** and **5** was known to be very laborious, we decided to postpone the separation after the cleavage of the ester function. A mixture of *cis* and *trans* ester **5** was subjected to the saponification reaction; surprisingly, the *cis*-**6** acid was obtained from this reaction, with almost no *trans*-**6** derivative being present. To understand this observation, the reaction was followed via NMR. The ¹H-NMR spectra of this reaction after 2 h and 3 days are shown in Figure 1. The integral of the respective *trans*-**6** $CH_{1,cyclohexyl}$ shows deterioration from approximately 30%–5% in relation to *cis*-**6**. After 3 days, no further changes in the isomer ratio were observed. Under basic conditions, an enol tautomer is formed, leading to an sp^2 -hybridized carbon at the C-1 of the cyclohexyl ring (**I**) (Figure 2). This allows the interconversion of **II** into **III** and vice versa. Due to 1,3-repulsion in **II**, the equilibrium shifts towards the thermodynamically more stable **III**. By conducting the ester cleavage without separating the *cis*- and *trans*-isomer, the *cis*-**6** was obtained in nearly 95% purity, while Romanelli et al. carefully separated the *trans* ester from the mixture ahead of the saponification reaction losing significant quantities of the desired compound in the process.



SCHEME 1 ^aSynthesis of *cis*-configured carboxylic acid **6** according to Romanelli et al.^[10] Reagents and conditions: (a) KOtBu, DMSO, rt, overnight; (b) MeOH, Pd/C, H₂ (1 bar); (c) NaOH, MeOH, rt, overnight. Synthesis of *cis*-**6** as conducted in this work. Reagents and conditions: (a) NaH, DMSO, 75°C to rt; 3 days. (b) EtOH, Pd/C, H₂ (1 bar), rt, 4 days; (c) NaOH, MeOH, rt, 3 days.

The subsequent reactions were performed applying the reported conditions^[10] (Scheme 2). Conversion of carboxylic acid *cis*-6 into the primary amine *cis*-7 was achieved via Curtius rearrangement. The amine *cis*-7 was subsequently alkylated using the bromoalkyl derivative 8 and a mixture of formaldehyde in formic acid. Simply by allowing the interconversion of *trans*-6 into *cis*-6 under basic conditions, the overall yield could be increased from 2% to 14%, allowing the preparation of the HCN channel blocker EC18 (*cis*-1) in a 600 mg scale.

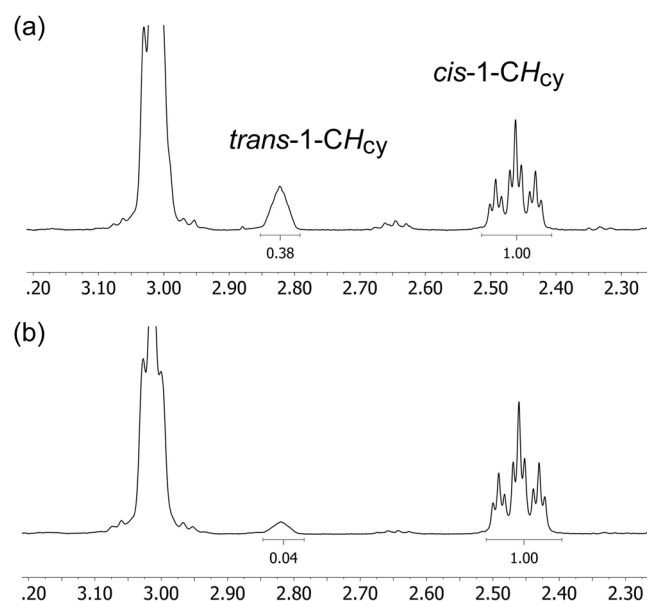


FIGURE 1 Section of NMR spectra of compound 6 displaying the signals for *trans* and *cis* 1-CH_{cyclohexyl} after 2 h (a) and after 3 d (b) under basic conditions (NaOH 2.5 M in MeOH).

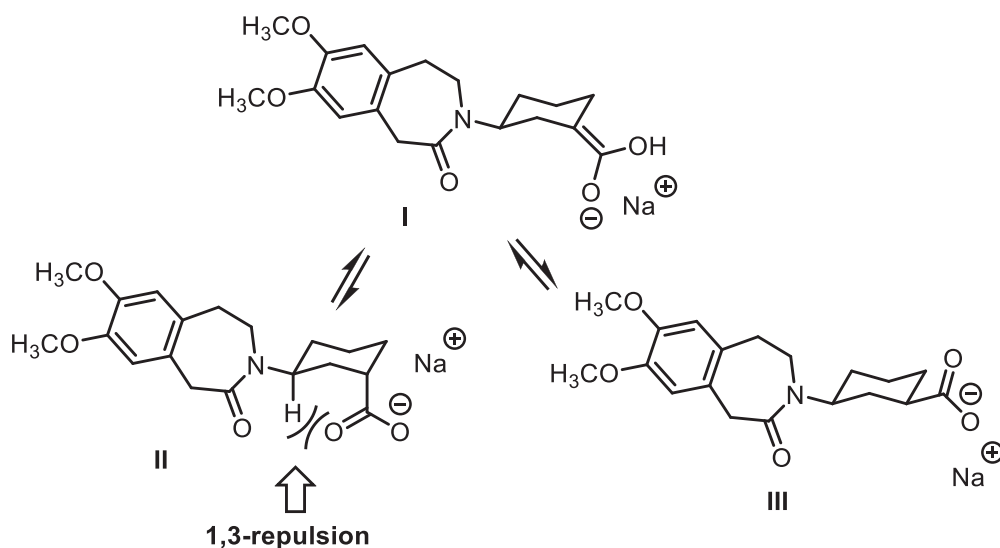


FIGURE 2 The postulated mechanism for interconversion of *trans*-6 (II) into *cis*-6 (III).

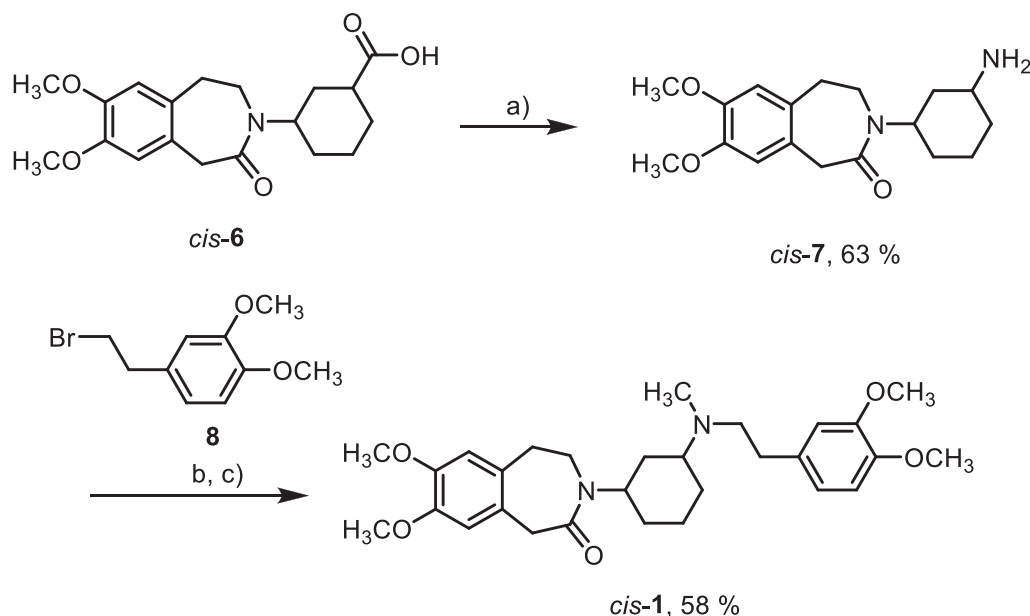
2.2 | Biological activity

2.2.1 | EC18 abolishes HCN4 triggered pace making in a human iPSC (hiPSC) pacemaker model

First, we evaluated the activity of EC18 (*cis*-1) in a model of human iPSC-derived cardiomyocytes. Human iPSC-derived cardiomyocytes were analyzed for sufficient HCN4 expression after 35 days of maturation in the maturation medium. Therefore, immunofluorescence staining against HCN4 and the membrane marker N-cadherin was performed. The differentiated hiPSC-derived cardiomyocytes clearly expressed HCN4.^[11] Furthermore, immunofluorescence staining showed a strong localization of HCN4 at the cell membranes (Figure 3a). Contraction profiling was performed to characterize the contraction changes during β -adrenergic stimulation with isoprenaline. Isoprenaline led to an increase in the contraction frequency from basal (25.33 ± 2.29 bpm) to β -adrenergically stimulated condition (39.11 ± 2.71 bpm) at room temperature. Under these conditions, HCN4 channels are activated via direct cAMP-binding leading to accelerated depolarization and increased beating rate. Thus, the beating rhythm is highly dependent on the HCN4 function. Application of the HCN4 inhibitor EC18 (*cis*-1) at 100 μ M to the β -adrenergic stimulated cells led to an immediate reduction of contraction events down to a complete inhibition after 10 s (Figure 3b).

2.2.2 | Alterations of intrinsic properties of TC VB neurons following EC18 application

Next, we assessed the effect of the HCN4-preferring blocker EC18 (*cis*-1) on I_h current properties in TC VB



SCHEME 2 Synthesis of secondary EC18 (*cis*-1). Reagents and conditions: (a) see Romanelli et al.^[10] (b) DMF, K₂CO₃, DMF, 60°C, overnight; (c) see Romanelli et al.^[10]

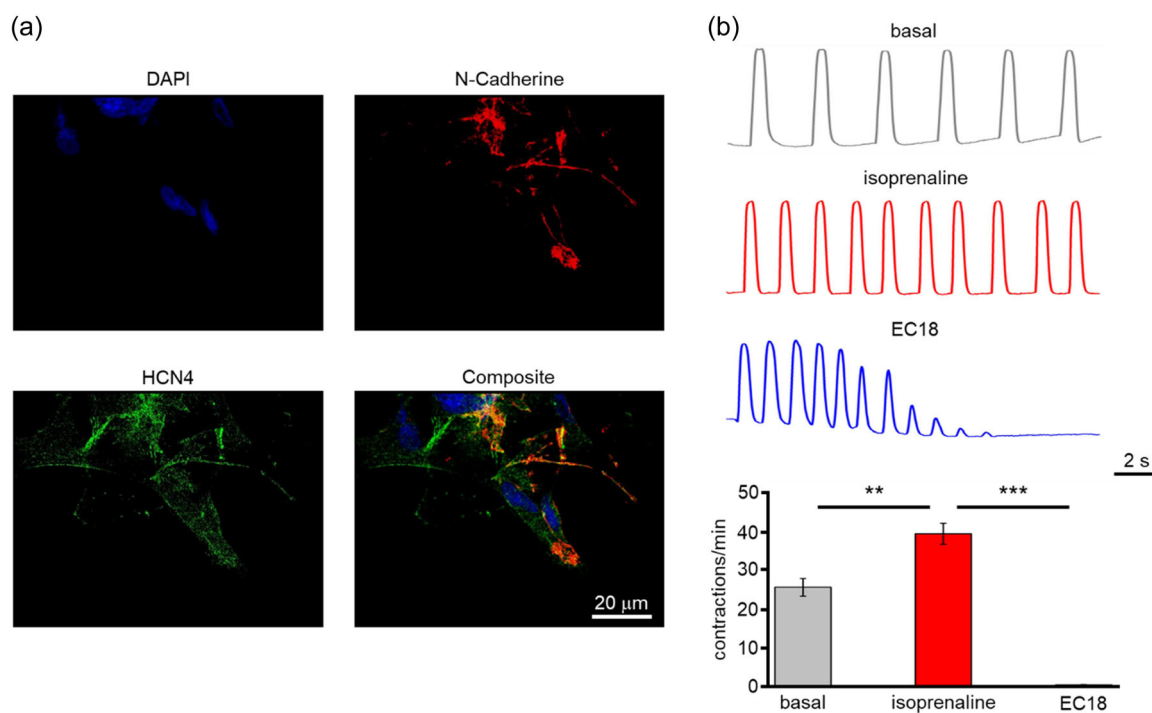


FIGURE 3 Effect of selective HCN4 blocker EC18 (*cis*-1) on rhythmic activity of human iPSC-derived pacemaker cells. (a) Immunofluorescence staining of HCN4 and the membrane marker N-Cadherine. (b) Pacemaker cells' rhythmic contraction was assayed via the muscle motion plugin for ImageJ Fiji. Application of isoprenaline (red exemplary trace) or isoprenaline plus EC18 (blue exemplary trace) resulted in an increased beating rate or almost completely abolished beating, respectively ($n = 10$). ** $p = 0.01$; *** $p = 0.001$.

neurons in C57BL/6J mice. Based on the expression of primarily HCN2 and HCN4 channel subunits in VB,^[2,13] these neurons are characterized by slowly activating large inward currents upon membrane hyperpolarization. To examine the I_h current in isolation, inward rectifier channels were blocked by adding

Ba²⁺ (0.5 mM) to the external aCSF. Voltage-dependent properties of I_h current were examined by whole-cell patch-clamp recordings.

Application of 30 μ M EC18 significantly reduced I_h current density in VB TC neurons for both sets of experiments (Set I, no

activation of I_h current during substance application; control: 9.98 ± 0.44 pA/pF, $n = 4$; EC18: 4.84 ± 0.89 pA/pF, $n = 4$; $p < 0.0001$; Set II, repetitive activation of I_h current during substance application: control: 12.45 ± 0.58 pA/pF, $n = 6$; EC18: 1.03 ± 0.98 pA/pF, $n = 6$; $p < 0.0001$; Figure 4a,b,e). However, the effect was more pronounced following repetitive activation of HCN channels during EC18 application (Set I: EC18: 4.80 ± 0.89 pA/pF, $n = 4$; Set II: EC18: 1.03 ± 0.98 pA/pF, $n = 6$; $p < 0.002$). These findings point to a use-dependent block of HCN channels by EC18 application (Figure 4c) as it could already be demonstrated for HCN4 overexpressing HEK-293 cells.^[14] Comparing the current densities of evoked currents at different time points during drug application revealed an increasing channel block. While the reduction was small after 5 min (0 min: 9.39 ± 0.71 pA/pF $n = 6$ vs. 5 min: 8.60 ± 0.74 pA/pF $n = 6$; $p > 0.6$), it became visible after 10 min (5 min: 8.60 ± 0.74 pA/pF $n = 6$ vs.

10 min: 5.87 ± 0.29 pA/pF $n = 6$; $p < 0.001$). At later time points, the effect was further increased (10 min: 5.87 ± 0.29 pA/pF $n = 6$ vs. 15 min: 2.43 ± 0.31 pA/pF $n = 6$; $p < 0.0002$) and was maximal after 20 min (15 min: 2.43 ± 0.31 pA/pF $n = 6$ vs. 15 min: 2.43 ± 0.31 pA/pF $n = 6$; $p = 0.197$) (Figure 4f).

Since the resting membrane potential (RMP) of TC neurons is regulated by other ion channels besides HCN channels,^[7] RMP of recorded VB neurons was compared between the different recording conditions (in the presence of 0.5 mM Ba^{2+}). No significant differences were found between the two sets of experiments (Set I: control: -66.00 ± 1.41 mV $n = 4$ vs. EC18: -63.00 ± 2.89 mV $n = 4$; $p > 0.05$; Set II: control: -60.50 ± 1.67 mV $n = 6$ vs. EC18: -64.00 ± 2.00 mV $n = 6$; $p > 0.05$) (Figure 4g). Moreover, it seems that the application of EC18 does not significantly change the half-maximal point of activation of HCN channels in either experimental

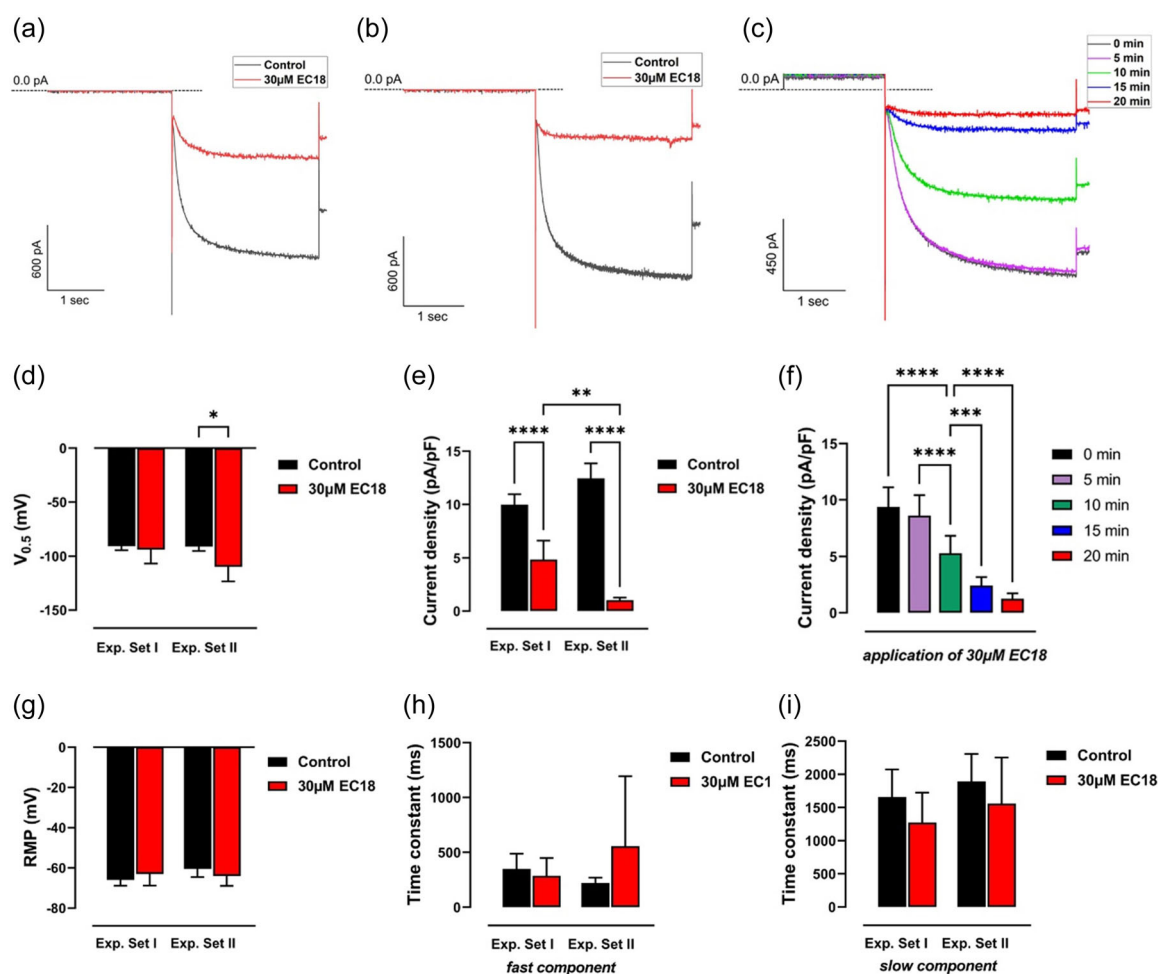


FIGURE 4 Effect of selective HCN4 blocker EC18 (*cis-1*) on I_h current recorded in thalamic neurons (a, b). Exemplary traces of I_h current recorded in TC VB neurons in the absence (in black) and presence of 30 μ M EC18 (in red) for Set I (a) and Set II (b). For clarity only, the hyperpolarizing step to -130 mV is shown. (c) Exemplary traces of I_h current at -110 mV were recorded by repetitive activation of HCN channels under control conditions (0 min; in black) and different time points following 30 μ M compound application (5 min in purple; 10 min in green; 15 min in blue; 20 min in red). (d–i) Bar graphs displaying $V_{0.5}$ (d), current density (e), resting membrane potential (RMP) (g), and both fast (h) and slow (i) components of activation kinetics before (in black) and after (in red) application of compound for both experimental set (Exp. Set I, II). (f) Bar graphs displaying the time-dependent decrease in current density following compound application. * $p = 0.01$; ** $p = 0.001$; *** $p = 0.0001$; **** $p = 0.00001$.

condition (Set I: control: -90.81 ± 1.78 mV $n=4$ vs. EC18: -93.78 ± 6.45 mV $n=4$; $p > 0.05$; Set II: control: -91.09 ± 1.61 mV $n=6$ vs. EC18: -109.9 ± 5.54 mV $n=6$; $p > 0.0407$) (Figure 4d). However, it seems that repetitive activation of HCN channels during the compound application does modify the slope of the steady-state activation curve (Figure 7d, experimental section).

Analysis of activation kinetics of recorded I_h current showed that despite major changes in current density due to EC18 application (Figure 4e), the two-time constants of activation kinetic revealed no significant differences after compound application in both sets of the experiment. For fast component (Figure 4h): (Set I: control: 349 ± 70 ms, $n=4$ vs. EC18: 287 ± 81 ms, $n=4$; $p > 0.05$; Set II: control: 220 ± 21 ms, $n=6$ vs. EC18: 556 ± 261 ms, $n=6$; $p > 0.05$) and for slow component (Figure 4i) (Set I: control: 1656 ± 209 ms, $n=4$ vs. EC18: 1275 ± 226 ms, $n=4$; $p > 0.05$; Set II: control: 1895 ± 169 ms, $n=6$ vs. EC18: 1560 ± 283 ms, $n=6$; $p > 0.05$).

Next, we assessed the dose-dependent inhibition of EC18 on I_h current in VB (Figure 5). To increase recording stability, the EC18 application was set to 15 min, and current steps to -110 mV were

applied and analyzed. Application of different concentrations of EC18 showed a clear dose-dependent reduction in I_h current density in VB TC neurons. While EC18 in a concentration of $0.1 \mu\text{M}$ had no effect (control: 8.48 ± 1.68 pA/pF, $n=2$; EC18: 9.13 ± 2.41 pA/pF, $n=2$; $p > 0.9$; Figure 5a,g), higher concentrations of $5 \mu\text{M}$ (control: 11.64 ± 0.80 pA/pF, $n=2$; EC18: 4.07 ± 2.19 pA/pF, $n=2$; $p = 0.056$; Figure 5b,g) and $10 \mu\text{M}$ (control: 11.70 ± 1.61 pA/pF, $n=3$; EC18: 5.26 ± 1.17 pA/pF, $n=3$; $p = 0.052$; Figure 5c,g) revealed visible inhibition. Saturating inhibition was found at $20 \mu\text{M}$ (control: 12.32 ± 1.79 pA/pF, $n=3$; EC18: 1.75 ± 0.59 pA/pF, $n=3$; $p < 0.001$; Figure 5d,g), $30 \mu\text{M}$ (control: 10.26 ± 1.07 pA/pF, $n=4$; EC18: 0.47 ± 0.23 pA/pF, $n=4$; $p < 0.001$; Figure 5e,g) and $100 \mu\text{M}$ (control: 11.91 ± 1.790 pA/pF, $n=3$; EC18: 1.205 ± 0.3270 pA/pF, $n=3$; $p < 0.001$; Figure 5f,g).

Next, activation kinetics of currents induced by hyperpolarizing steps to -110 mV were subjected to double exponential fitting. No significant differences were found for the time constant of the fast activation component ($0.1 \mu\text{M}$; control: 492 ± 149 ms, $n=2$ vs. EC18: 493 ± 162 ms, $n=2$; $p > 0.5$; $5 \mu\text{M}$; control: 301 ± 91 ms, $n=2$ vs. EC18: 246 ± 58 ms,

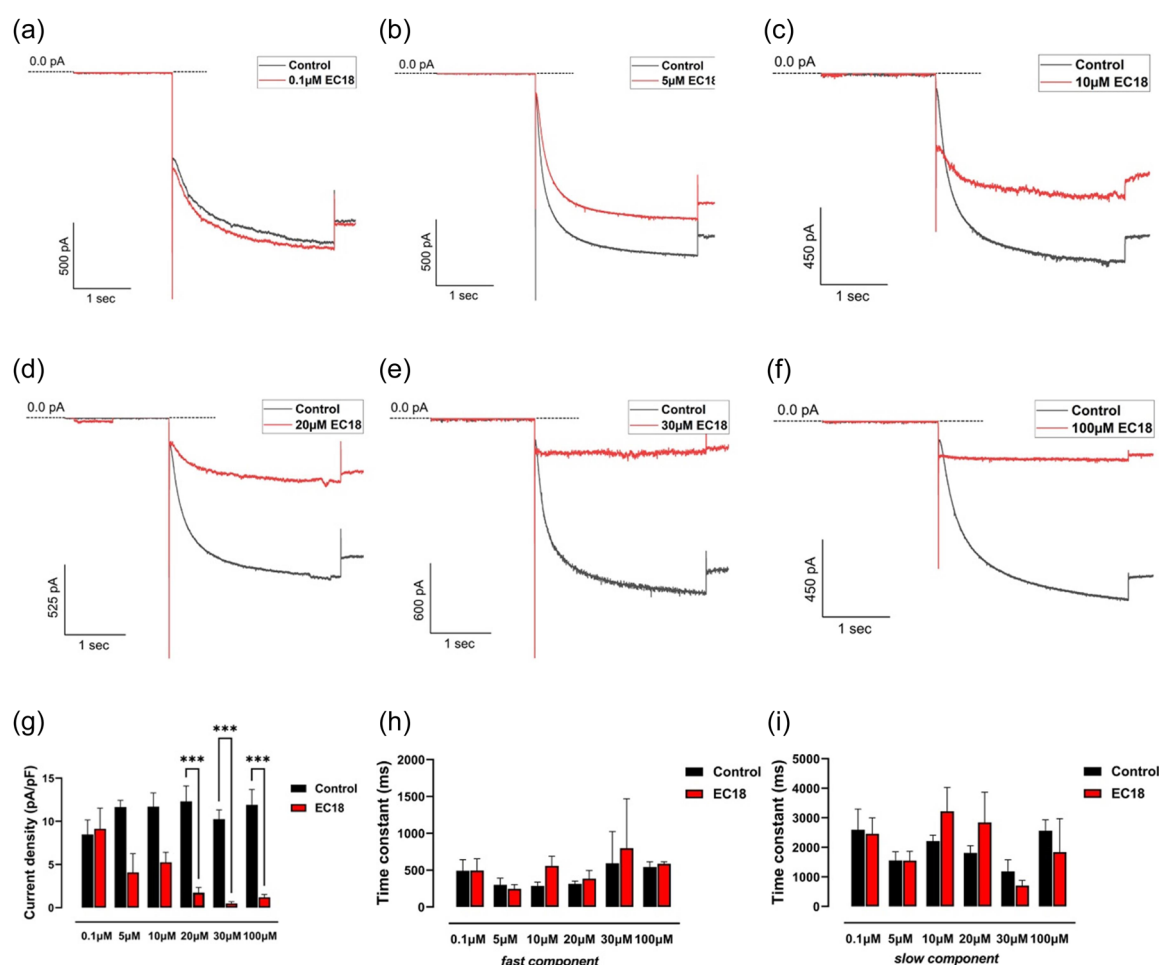


FIGURE 5 Dose-dependent effect of the selective HCN4 blocker EC18 (*cis-1*) on I_h current recorded in thalamic neurons. (a–f), Exemplary traces of I_h current were recorded in TC VB neurons in the absence (in black) and presence of EC18 (in red) for different concentrations of compound (as indicated). The hyperpolarizing step to -110 mV is shown. (g), current density and both fast (h) and slow (i) components of activation kinetics before (in black) and after (in red) application of the compound. *** $p = 0.0001$.

$n = 2$; $p > 0.5$; $10 \mu\text{M}$; control: $286 \pm 51 \text{ ms}$, $n = 3$ vs. EC18: $558 \pm 132 \text{ ms}$, $n = 3$; $p > 0.5$; $20 \mu\text{M}$; control: $315 \pm 38 \text{ ms}$, $n = 3$ vs. EC18: $383 \pm 113 \text{ ms}$, $n = 2$; $p > 0.5$; $30 \mu\text{M}$; control: $593 \pm 432 \text{ ms}$, $n = 4$ vs. EC18: $796 \pm 673 \text{ ms}$, $n = 4$; $p > 0.5$; $100 \mu\text{M}$; control: $543 \pm 71 \text{ ms}$, $n = 3$ vs. EC18: $586 \pm 28 \text{ ms}$, $n = 3$; $p > 0.5$; Figure 5h). Also for the time constant of the slow activation component, no significant differences were found ($0.1 \mu\text{M}$; control: $259 \pm 706 \text{ ms}$, $n = 2$ vs. EC18: $2459 \pm 541 \text{ ms}$, $n = 2$; $p > 0.5$; $5 \mu\text{M}$; control: $1557 \pm 296 \text{ ms}$, $n = 2$ vs. EC18: $1556 \pm 315 \text{ ms}$, $n = 2$; $p > 0.5$; $10 \mu\text{M}$; control: $2210 \pm 205 \text{ ms}$, $n = 3$ vs. EC18: $3219 \pm 809 \text{ ms}$, $n = 3$; $p > 0.5$; $20 \mu\text{M}$; control: $1811 \pm 247 \text{ ms}$, $n = 3$ vs. EC18: $2843 \pm 1023 \text{ ms}$, $n = 2$; $p > 0.5$; $30 \mu\text{M}$; control: $1190 \pm 391 \text{ ms}$, $n = 4$ vs. EC18: $706.3 \pm 182 \text{ ms}$, $n = 4$; $p > 0.5$; $100 \mu\text{M}$; control: $2562 \pm 373 \text{ ms}$, $n = 3$ vs. EC18: $1839 \pm 1137 \text{ ms}$, $n = 3$; $p > 0.5$; Figure 5i).

Our findings characterize EC18 (*cis-1*) as a potent inhibitor of I_h current in thalamic neurons that show properties of a use-dependent blocker that has no effect on activation kinetics.

2.2.3 | No influence on T lymphocyte activation through EC18

Lymphocytes include B cells, T cells, and natural killer cells and belong to the so-called “white blood cells.” The group of CD3+ T-lymphocytes comprises T-helper and T-killer cells that can be distinguished via their surface markers, CD4 and CD8, respectively. Those cell types are known key players in the pathogenesis of a variety of autoimmune diseases, among them MS.^[15] Here, we isolated primary splenocytes from naive mice, stimulated T cells by adding anti-CD3 and anti-CD28 antibodies, and checked whether the

application of EC18 (*cis-1*) affected T cell activation. CD25 and CD69 are lymphocytic surface markers and are expressed only on activated lymphocytes, with CD69 being an early and CD25 being a later activation marker.^[16,17]

Primary murine splenocytes were cultured in media with varying EC18 (*cis-1*) concentrations and their viability was checked. None of the tested EC18 treatments did affect the proportion of living cells (Figure 6a and 6b; unstim: 49.65 ± 4.1 ; $0 \mu\text{M}$: 70.06 ± 2.2 ; $0.1 \mu\text{M}$: 71.52 ± 1.7 ; $1 \mu\text{M}$: 73.35 ± 2.4 ; $5 \mu\text{M}$: 70.53 ± 1.8 ; $10 \mu\text{M}$: 67.95 ± 1.8). To examine the effect of the HCN4 channel blocker, EC18 (*cis-1*), on the activation of CD4+ and CD8+ T lymphocytes, the expression of the CD25 and CD69 was detected via flow cytometry (Figure 6a for an exemplary gating strategy). Neither CD4 (Figure 6c) nor CD8 (Figure 6d) positive T lymphocytes revealed altered expression of activation markers with EC18 treatment compared to control conditions (CD4+CD25+: unstim: 1.52 ± 0.4 ; $0 \mu\text{M}$: 51.21 ± 2.3 ; $5 \mu\text{M}$: 48.46 ± 2.0 ; CD4+CD69+: unstim: 0.4 ± 0.1 ; $0 \mu\text{M}$: 58.39 ± 2.9 ; $5 \mu\text{M}$: 56.15 ± 2.0 ; CD8+CD25+: unstim: 0.59 ± 0.1 ; $0 \mu\text{M}$: 34.28 ± 2.9 ; $5 \mu\text{M}$: 35.75 ± 4.0 ; CD8+CD69+: unstim: 0.24 ± 0.1 ; $0 \mu\text{M}$: 59.00 ± 4.9 ; $5 \mu\text{M}$: 57.11 ± 4.3). According to these experiments, we conclude that HCN4 channel inhibition via EC18 does not affect T lymphocyte activation.

2.2.4 | Off-target activity of EC18 at P2XR

Since the selectivity profile of EC18 (*cis-1*) was not evaluated across targets other than HCN channels, we have assessed the off-target

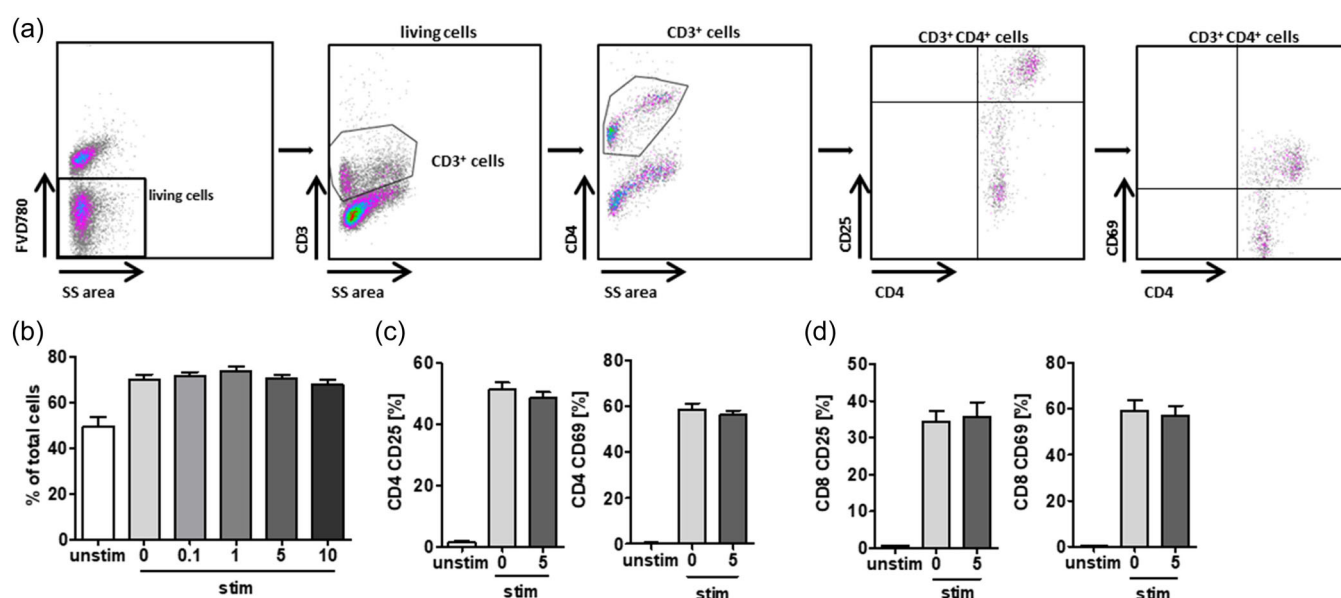


FIGURE 6 EC18 (*cis-1*) treatment has no impact on murine splenocyte viability and lymphocyte activation. (a) Exemplary gating strategy for the identification of CD3+CD4+CD25+ and CD69+ lymphocytes. (b) Quantification of viable splenocytes. Primary isolated splenocytes were stimulated with antibodies against CD3 and CD28 (stim, stimulated) or were left untreated (unstim, unstimulated). Stimulated splenocytes were incubated with different concentrations of EC18 (in μM). (c, d) Expression of activation markers CD25 and CD69 on CD3+CD4+CD3+CD8+ were not affected after EC18 treatment ($n = 4$).

activity of EC18 at a panel of P2X receptors: P2X1, P2X2, P2X2/3, P2X4, and P2X7 receptors. The compound did not display any antagonistic activity at P2X receptors at a concentration of 10 μM .

3 | CONCLUSION

EC18 (*cis*-1) is one of the few subtype-preferring HCN channel inhibitors and was proposed as a promising tool compound for investigating the HCN4 channel function. Indeed EC18 acts as a potent HCN4 inhibitor in a human iPSC-derived sinus node model with proven HCN4 expression.^[11] However, off-target effects on other channels like Na^+ channels or Ca^{2+} channels cannot be fully excluded.

In brain tissue application of EC18 (*cis*-1) at a concentration of 30 μM revealed that the compound significantly reduced I_h current in TC VB neurons in acute brain slices of C57BL/6J mice (Figure 4a–c,e) without affecting other current properties including voltage dependence (but see: Exp. Set I, Figure 4d) and activation kinetics (Figure 4h,i). Under the present recording conditions, that is, block of several sustained K^+ channels by Ba^{2+} , the resting membrane potential is confounded and shifted to more depolarized potentials. Consequently, HCN channels do not significantly contribute to the resting membrane potential, and EC18 (*cis*-1) has no effect under current clamp conditions (Figure 4g). Under voltage clamp conditions, the two sets of the experiment differ with respect to the repetitive activation of HCN channels during EC18 application. The stronger reduction of I_h current density by EC18 (*cis*-1) during Set II (Figure 4e) is therefore not only based on the duration of substance application but also on the frequency of HCN channel activation during compound application. In accordance with the formerly published results,^[10] we found that the inhibition of I_h current density by EC18 is dose-dependent with no effects on current kinetics. Inhibition is visible at low concentrations, such as 5 μM , and mostly complete at 30 μM .

Our data furthermore indicates no functional involvement of HCN4 channels in the activation of murine CD4+ and CD8+ T cells.

4 | EXPERIMENTAL

4.1 | Chemistry

4.1.1 | General

Unless otherwise noted, moisture-sensitive reactions were conducted under dry nitrogen. Flash column chromatography (fc): Silica gel 60, 40–64 μm ; parentheses include: diameter of the column, length of the column, fraction size, eluent, R_f value. Melting point: melting point apparatus Stuart Scientific[®] SMP 3, uncorrected. IR: IR spectrophotometer FT-ATR-IR (Jasco[®]). ^1H NMR (400 MHz): Unity Mercury Plus 400 spectrometer (Varian[®]), AV400 (Bruker[®]), JEOL AJNM-ECA-400. ^{13}C NMR (100 MHz): Unity Mercury plus 400

spectrometer (Varian[®]) JEOL JNM-ECA-400; δ in ppm relative to tetramethylsilane; coupling constants are given with 0.5 Hz resolution, the assignments of ^{13}C and ^1H NMR signals were supported by 2D NMR techniques; MS: APCI = atmospheric pressure chemical ionization, EI = electron impact, ESI = electro-spray ionization: Micro-Tof (Bruker Daltronics, Bremen), calibration with sodium formate clusters before measurement. All solvents were of analytical grade quality and demineralized water was used. HPLC solvents were of gradient-grade quality, and ultrapure water was used. All HPLC eluents were degassed by sonication before use. Thin-layer chromatography was conducted with silica gel F₂₅₄ on aluminum plates in a saturated chamber at room temperature. The spots were visualized using UV light (254 nm) or reagents such as a cerium molybdate dipping bath with additional heating using a standard heat gun. Hence the retention factor values strongly depend on the temperature, the chamber saturation, and the exact ratio of components of the eluent (highly volatile); the given retention factor values represent just approximate values. Flash column chromatography was conducted with silica gel 600 (40–63 μm , Macherey-Nagel).

4.1.2 | HPLC purity measurements

Equipment: UV-detector: UltiMate 3000 variable Wavelength Detector; autosampler: UltiMate 3000; pump: Ultimate 3000; degasser: Ultimate 3000; data acquisition: Chromeleon Client 8.0.0 (Dionex Corpor.). Method: column: guard column: Zorbax SB-Aq 12.5 \times 4.6 mm cartridge, column: Zorbax SB-Aq StableBond analytical 150 \times 4.6 mm, flow rate: 1.00 mL/min; injection volume: 5.0 μL ; detection at λ = 210 nm.

Method A: solvents: A: Tetrabutylammonium phosphate buffer (5 mM) in H_2O , B: CH_3CN , gradient elution: (A %): 0–20 100% to 90%, 20–30 min: gradient from 90% to 100%.

Method B: solvents: A: Tetrabutylammonium phosphate buffer (5 mM) in H_2O , B: CH_3CN , gradient elution: (A %): 0–20 min 80% to 20%, 20–30 min: gradient from 20% to 80%.

Method C: solvents: A: Tetrabutylammonium phosphate buffer (5 mM) in H_2O , B: CH_3CN , gradient elution: (A %): 40%–100%, 20–30 min: gradient from 100% to 40%.

4.1.3 | Data analysis

NMR spectra were processed with MestReNova 12.0 (MestreLab Research) and are provided as Supporting Information.

cis-3-{3-[2-(3,4-Dimethoxyphenyl)ethyl](methyl)amino)cyclohexyl}-7,8-dimethoxy-1,3,4,5-tetrahydro-2H-benzo[d]azepin-2-one (*cis*-1)

cis-3-(3-Aminocyclohexyl)-7,8-dimethoxy-1,3,4,5-tetrahydro-2H-benzo[d]azepin-2-one (*cis*-7, 150 mg, 0.47 mmol, 1 eq) was dissolved in dry dimethyl formamide (2 mL) under N_2 atmosphere and K_2CO_3

(195 mg, 1.41 mmol, 3 eq) was added. 4-(2-Bromoethyl)-1,2-dimethoxybenzene (**8**, 127 mg, 0.52 mmol, 1.1 eq) was dissolved in dry dimethyl formamide (1 mL) and added slowly over a period of 1 h to the reaction mixture. The mixture was heated to 60°C and was stirred overnight. The mixture was cooled to room temperature, diluted with a saturated solution of NaHCO₃ (20 mL), and extracted with CH₂Cl₂ (3 × 30 mL). The combined organic layers were washed with brine (5 mL), dried over Na₂SO₄, filtered, and concentrated in vacuo. The crude product was purified via flash chromatography (CH₂Cl₂ + 5% H₃COH + 0.5% NH₄OH, Ø = 3 cm, *h* = 14 cm, *V* = 20 mL) to yield 138 mg of a light yellow oil (C₂₈H₃₈N₂O₅, 482.62 g/mol, 0.28 mmol, 61%). TLC (Silica): *R*_f = 0.36 (CH₂Cl₂ + 5% H₃COH + 0.5% NH₄OH). Exact mass (APCI): *m/z* = calcd. for C₂₈H₃₉N₂O₅ [M+H⁺] 483.2854, found 483.2810. ¹H NMR (400 MHz, CDCl₃): δ = 6.83–6.77 (m, 1H, 5-CH₂dimethoxyphenyl), 6.76–6.70 (m, 2H, 2-CH₂dimethoxyphenyl, 6-CH₂dimethoxyphenyl), 6.59 (s, 1H, 9-CH₂benzazepinone), 6.52 (s, 1H, 6-CH₂benzazepinone), 4.58–4.45 (m, 1H, 1-CH₂cyclohexyl), 3.88–3.79 (m, 14H, 7-CH₃O_{benzazepinone}, 8-CH₃O_{benzazepinone}, 3-CH₃O-3_{dimethoxyphenyl}, 4-CH₃O_{dimethoxyphenyl}, 1-CH₂benzazepinone), 3.70–3.60 (m, 2H, 4-CH₂benzazepinone), 3.03–2.97 (m, 2H, 5-CH₂benzazepinone), 2.98–2.90 (m, 2H, NHCH₂CH₂), 2.90–2.78 (m, 2H, NHCH₂CH₂ethyl), 2.80–2.60 (m, 1H, 3-CH₂cyclohexyl), 2.14–1.01 (m, 8H, 2-CH₂cyclohexyl, 4-CH₂cyclohexyl, 5-CH₂cyclohexyl, 6-CH₂cyclohexyl). ¹³C NMR (101 MHz, CDCl₃): δ = 172.1 (1C, C=O_{benzazepinone}), 149.0 (1C, C-3_{dimethoxyphenyl}), 147.9 (1C, C-7_{benzazepinone}), 147.6 (1C, C-4_{dimethoxyphenyl}), 147.1 (1C, C-8_{benzazepinone}), 131.50 (1C, C-1_{dimethoxyphenyl}, signal only visible in gHMBC), 127.1 (1C, C-5a_{benzazepinone}), 123.3 (1C, C-9a_{benzazepinone}), 120.5 (1C, C-6_{dimethoxyphenyl}), 114.0 (1C, C-9_{benzazepinone}), 113.2 (1C, C-6_{benzazepinone}), 111.9 (1C, C-2_{dimethoxyphenyl}), 111.4 (1C, C-5_{dimethoxyphenyl}), 56.1 (1C, C-3_{cyclohexyl}), 55.92, 55.91 and 55.88 (4C, CH₃O-7_{benzazepinone}, CH₃O-8_{benzazepinone}, CH₃O-3_{dimethoxyphenyl}, CH₃O-4_{dimethoxyphenyl}), 50.6 (1C, C-1_{cyclohexyl}), 48.0 (1C, NHCH₂), 43.0 (1C, C-1_{benzazepinone}), 40.3 (1C, C-4_{benzazepinone}), 36.8 (1C, C-2_{cyclohexyl}), 35.2 (1C, NHCH₂CH₃), 33.9 (1C, C-5_{benzazepinone}), 31.9 (1C, C-4_{cyclohexyl}), 29.9 (1C, C-6_{cyclohexyl}), 23.0 (1C, C-5_{cyclohexyl}). FTIR (neat): $\tilde{\nu}$ (cm⁻¹) = 2980, 2970 (C-H_{aliph}), 1608 (C=O), 1516 (C=C_{arom}).

cis-(3-[3-[2-(3,4-Dimethoxyphenyl)ethyl]amino]cyclohexyl)-7,8-dimethoxy-1,3,4,5-tetrahydro-2H-benzazepin-2-one (*cis*-**126**, 292 mg, 0.61 mmol, 1 eq) was dissolved in ethanol (10 mL). Formaldehyde (245 mg, 3.03 mmol, 5 eq) and formic acid (562 mg, 12.2 mmol, 20 eq) were added and the mixture was heated to 80°C for 3.5 h. The solution was cooled to room temperature and stirred overnight. The solvent was removed in vacuo and a saturated solution of Na₂CO₃ (15 mL) was added. The aqueous mixture was extracted with ethyl acetate (3 × 40 mL), the combined organic layers were dried over Na₂SO₄, filtered and the solvent was removed in vacuo. The crude product was purified via flash chromatography (CH₂Cl₂ + 5% H₃COH + 0.5% NH₄OH, Ø = 2.5 cm, *h* = 15 cm, *V* = 20 mL). Next diethyl ether (3 mL) was added to the isolated product, the solvent was evaporated by applying an airflow over the flask and the residue was dried in a high vacuum to yield 290 mg of a colorless solid (C₂₉H₄₀N₂O₅, 496.65 g/mol, 0.58 mmol, 96%). TLC

(Silica): *R*_f = 0.71 (CH₂Cl₂ + 5% H₃COH + 0.5% NH₄OH). mp: 68°C. Exact mass (APCI): *m/z* = calcd. for C₂₉H₄₁N₂O₅ [M+H⁺] 497.3001, found 497.2963 Purity (HPLC, method Purity A): 94%, *R*_t = 12.8 min. ¹H NMR (400 MHz, CDCl₃): δ = 6.79 (d, *J* = 8.7 Hz, 1H, 5-CH₂dimethoxyphenyl), 6.75–6.70 (m, 2H, 2-CH₂dimethoxyphenyl, 6-CH₂dimethoxyphenyl), 6.59 (s, 1H, 9-CH₂benzazepinone), 6.52 (s, 1H, 6-CH₂benzazepinone), 4.56–4.36 (m, 1H, 1-CH₂cyclohexyl), 3.92–3.78 (m, 14H, 7-CH₃O_{benzazepinone}, 8-CH₃O_{benzazepinone}, CH₃OC-3_{dimethoxyphenyl}, CH₃OC-4_{dimethoxyphenyl}, 1-CH₂benzazepinone), 3.72–3.62 (m, 2H, 4-CH₂benzazepinone), 3.04–2.96 (m, 2H, 5-CH₂benzazepinone), 2.83–2.59 (m, 5H, 3-CH₂cyclohexyl, NHCH₂, NHCH₂CH₃), 2.39 (s, 3H, NCH₃), 1.97–1.80 (m, 3H, 2-CHH_{cyclohexyl}, 4-CHH_{cyclohexyl}, 5-CHH_{cyclohexyl}), 1.71 (d, *J* = 10.7 Hz, 1H, 6-CHH_{cyclohexyl}), 1.49–1.28 (m, 3H, 2-CHH_{cyclohexyl}, 5-CHH_{cyclohexyl}, 6-CHH_{cyclohexyl}), 1.28–1.18 (m, 1H, 4-CHH_{cyclohexyl}). ¹³C NMR (101 MHz, CDCl₃): δ = 172.1 (1C, C=O_{benzazepinone}), 149.0 (1C, C-3_{dimethoxyphenyl}), 148.0 (1C, C-7_{benzazepinone}), 147.6 (1C, C-4_{dimethoxyphenyl}), 147.3 (1C, C-8_{benzazepinone}), 132.8 (1C, C-1_{dimethoxyphenyl}), 127.3 (1C, C-5a_{benzazepinone}), 123.5 (1C, C-9a_{benzazepinone}), 120.7 (1C, C-6_{benzazepinone}), 114.2 (1C, C-9_{benzazepinone}), 113.3 (1C, C-6_{benzazepinone}), 112.2 (1C, C-2_{dimethoxyphenyl}), 111.4 (1C, C-5_{dimethoxyphenyl}), 61.7 (1C, C-3_{cyclohexyl}), 56.2 (1C, NHCH₂CH₃), 56.07, 56.04 and 56.03 (4C, CH₃O-7_{benzazepinone}, CH₃O-8_{benzazepinone}, CH₃O-3_{dimethoxyphenyl}, CH₃O-4_{dimethoxyphenyl}), 51.8 (1C, C-1_{cyclohexyl}), 43.2 (1C, C-1_{benzazepinone}), 40.7 (1C, C-4_{benzazepinone}), 37.9 (1C, NCH₃), 34.1 (1C, C-5_{benzazepinone}), 33.9 (1C, NHCH₂CH₃), 32.28 (1C, C-2_{cyclohexyl}), 30.3 (1C, C-6_{cyclohexyl}), 28.4 (1C, C-4_{cyclohexyl}), 23.6 (1C, C-5_{cyclohexyl}). FTIR (neat): $\tilde{\nu}$ (cm⁻¹) = 2980, 2970, 2931 (C-H), 1643 (C=O), 1514 (C=C_{arom}).

Ethyl 5-bromocyclohex-3-ene-1-carboxylate (**2b**)

Cyclohex-3-ene-1-carboxylic acid (1 eq, 47.56 mmol, 6 mL) was dissolved in ethanol (abs., 30 mL) and H₂SO₄ (conc., 0.1 mL) was added. The mixture was heated to reflux for 3 h and the solvent was removed in vacuo. A saturated solution of K₂CO₃ (20 mL) was added and the mixture was extracted using ethyl acetate (2 × 30 mL). The organic layer was washed with brine (5 mL) and the solvent was concentrated in vacuo until a volume of ca. 3 mL remained. Then CH₂Cl₂ (20 mL) was added, and the solvent was removed completely in vacuo to yield 7.28 g of brown oil (C₉H₁₄O₂, 154.21 g/mol, 47.22 mmol, quant.) TLC (Silica): *R*_f = 0.89 (ethyl acetate/cyclohexane = 1:4). Exact mass (ESI): *m/z* = calcd. for C₉H₁₅O₂ [M+H⁺] 155.1067, found 155.1066. ¹H NMR (400 MHz, CDCl₃): δ (ppm) = 5.67 (s, 2H, 3-CH_{cyclohexene}, 4-CH_{cyclohexene}), 4.13 (qd, *J* = 7.1, 0.5 Hz, 2H, OCH₂), 2.53 (m, 1H, 1-CH_{cyclohexene}), 2.28–2.19 (m, 2H, 2-CH₂), 2.13–2.04 (m, 2H, 5-CH₂), 2.04–1.94 (m, 1H, 6-CHH), 1.74–1.60 (m, 1H, 6-CHH), 1.25 (t, *J* = 7.1 Hz, 3H, CH₃). ¹³C NMR (600 MHz, CDCl₃): δ (ppm) = 176.0 (1C, C=O_{ester}), 126.8 and 125.4 (2C, C-3_{cyclohexene}, C-4_{cyclohexene}), 60.4 (1C, OCH₂), 39.5 (1C, C-1_{cyclohexene}), 27.6 (1C, C-2_{cyclohexene}), 25.2 (1C, C-6_{cyclohexene}), 24.6 (1C, C-5_{cyclohexene}), 14.4 (3C, CH₃). FTIR (neat): $\tilde{\nu}$ (cm⁻¹) = 2980, 2930 (C-H), 1732 (C=O).

Ethyl cyclohex-3-ene-1-carboxylate (3.00 g, 19.5 mmol, 1 eq) was dissolved in CCl₄ (5 mL) and *N*-bromo succinimide (4.16 g, 23.4 mmol, 1.2 eq) and azobisisobutyronitrile (1–2 mg) were added.

The mixture was heated to 75°C and stirred for 3 h. The temperature was then increased to reflux and the mixture was stirred for an additional 1 h. The mixture was filtered, and the solvent of the filtrate was concentrated in vacuo. The mixture was filtered again, and the filtrate was concentrated in vacuo to yield 4.32 g of brown oil, $C_9H_{13}BrO_2$ (233.11 g/mol, 18.5 mmol, 95%). TLC (Silica): R_f = 0.25 (cyclohexane/ethyl acetate = 9:1). Exact mass (APCI): m/z = calcd. for $C_9H_{13}^{79}BrO_2$ [$M+H^+$] 233.0172, found 233.0156. 1H NMR (400 MHz, $CDCl_3$): δ = 6.12–5.71 (m, 2H, 3- $CH_{cyclohexenyl}$, impurity*), 4.93–4.84 (m, 1H, 5- $CH_{cyclohexenyl}$), 4.78 (m, impurity*), 4.16 (q, J = 7.2 Hz, 2H, OCH_2CH_3), 3.29–3.15 (m, impurity*), 3.04 (m, 1H, 1- $CH_{cyclohexenyl}$), 2.59–1.95 (m, 4H, 2- $CH_{2,cyclohexenyl}$, 6- $CH_{2,cyclohexenyl}$), 1.27 (t, J = 7.0 Hz, 3H, OCH_2CH_3). ^{13}C NMR (101 MHz, $CDCl_3$): δ = 174.8 (1C, $C=O_{ester}$), 128.9 and 128.4 (2C, C-3, -4 $_{cyclohexenyl}$), 60.7 (1C, OCH_2CH_3), 46.9 (1C, C-5 $_{cyclohexenyl}$), 35.1 (1C, C-1 $_{cyclohexenyl}$), 34.4 (1C, C-6 $_{cyclohexenyl}$), 27.5 (1C, C-2 $_{cyclohexenyl}$), 14.2 (1C, OCH_2CH_3). FTIR (neat): $\tilde{\nu}$ (cm^{-1}) = 2890 (C-H $_{aliph}$), 1728 (C=O).

7,8-Dimethoxy-1,3-dihydro-2H-benzo[d]azepin-2-one (3)

3,4-Dimethoxyphenylacetic acid (20.00 g, 101.9 mmol, 1 eq) was suspended in dry CH_2Cl_2 under an N_2 atmosphere. $SOCl_2$ (22 mL) was added, and the mixture was heated to 42°C for 1 h. The mixture was then heated to 80°C and the solvent and $SOCl_2$ were distilled off in vacuo. The residue was dissolved in dry CH_2Cl_2 (50 mL) and the mixture was cooled to 0°C. Aminoacetaldehyde dimethyl acetal (10.7 mL, 102 mmol, 1 eq) was dissolved in dry CH_2Cl_2 (100 mL), triethylamine (20 mL) was added and the resulting solution was added slowly to the reaction mixture. The mixture was allowed to warm up to room temperature and was stirred overnight. The mixture was subsequently washed with a solution of $NaHCO_3$ (saturated solution, diluted 1:6 with water, 3 \times 50 mL), $NaHCO_3$ (saturated solution, diluted 1:1 with water, 2 \times 50 mL), and brine (2 \times 20 mL), then combined aqueous layers were extracted using CH_2Cl_2 . The organic layers were combined, dried over Na_2SO_4 , and filtered and the solvent was removed in vacuo to yield 26.3 g of the off-white solid ($C_{14}H_{21}NO_5$, 283.32 g/mol, 92.8 mmol, 91%). TLC (Silica): R_f = 0.25 (cyclohexane/ethyl acetate = 1:1 + 5% H_3COH). mp: 62°C. Exact mass (APCI): m/z = calcd. for $C_{14}H_{22}NO_5$ [$M+H^+$] 284.1492, found 284.1461. Purity (HPLC, method Purity B): 78%, R_t = 5.7 min. 1H NMR (400 MHz, $CDCl_3$): δ = 6.83 (d, J = 8.5 Hz, 1H, 5- $CH_{dimethoxyphenyl}$), 6.80–6.75 (m, 2H, 2-, 6- $CH_{dimethoxyphenyl}$), 5.65 (s, 1H, NH), 4.31 (t, J = 5.3 Hz, 1H, $CH(OCH_3)_2$), 3.87 (s, 6H, 3- $CH_3OC_{dimethoxyphenyl}$, 4- $CH_3OC_{dimethoxyphenyl}$), 3.51 (s, 2H, $PhCH_2CO$), 3.39–3.28 (m, 8H, $CH(OCH_3)_2$, $NHCH_2CH$). ^{13}C NMR (101 MHz, $CDCl_3$): δ = 171.6 (1C, $C=O$), 149.4 and 148.5 (2C, C-3, -4 $_{dimethoxyphenyl}$), 127.4 (1C, C-1 $_{dimethoxyphenyl}$), 121.7 (1C, C-6 $_{dimethoxyphenyl}$), 112.5 (1C, C-2 $_{dimethoxyphenyl}$), 111.7 (1C, C-5 $_{dimethoxyphenyl}$), 102.7 (1C, $CH(OCH_3)_2$), 56.1 and 56.0 (2C, CH_3O -3 $_{dimethoxyphenyl}$, CH_3O -4 $_{dimethoxyphenyl}$), 54.6 (2C, $CH(OCH_3)_2$), 43.4 ($PhCH_2CO$), 41.2 (1C, $NHCH_2CH$). FTIR (neat): $\tilde{\nu}$ (cm^{-1}) = 3293 (N-H), 2981, 2967, 2924 (C-H $_{aliph}$), 1645 (C=O), 1514 (C=C $_{arom}$).

N-(2,2-Dimethoxyethyl)-2-(3,4-dimethoxyphenyl)acetamide (10.0 g, 35.3 mmol, 1 eq) was dissolved in a mixture of hydrochloric

acid and acetic acid (1:1, 100 mL) and the solution was stirred at room temperature for 1 day. The solution was poured onto a mixture of water and ice (1:1, 120 mL) and an off-white solid was formed, which was filtered off and dried at 70°C for 3 h to yield 26.3 g of colorless solid ($C_{12}H_{13}NO_3$, 219.24 g/mol, 23.0 mmol, 65%). TLC (Silica): R_f = 0.46 (cyclohexane/ethyl acetate = 1:9). mp: 245°C. Exact mass (APCI): m/z = calcd. for $C_{12}H_{13}NO_3$ [$M+H^+$] 220.0968, found 220.0961. Purity (HPLC, method Purity B): >99%, R_t = 6.65 min. 1H NMR (400 MHz, $CDCl_3$): δ = 7.69 (s, 1H, 9- $CH_{benzazepinone}$), 7.66 (s, 1H, 6- $CH_{benzazepinone}$), 7.05 (d, J = 9.1 Hz, 1H, 5- $CH_{benzazepinone}$), 6.99 (dd, J = 9.1, 4.7 Hz, 1H, 4- $CH_{benzazepinone}$), 4.58 (s, 3H, 8- $CH_3O_{benzazepinone}$), 4.55 (s, 3H, 7- $CH_3O_{benzazepinone}$), 4.13 (s, 2H, NH), 4.09 (s, 2H, 1- $CH_{2,benzazepinone}$). ^{13}C NMR (101 MHz, $CDCl_3$): δ = 178.1 (1C, $C=O_{benzazepinone}$), 158.6 (1C, C-8 $_{benzazepinone}$), 157.1 (1C, C-7 $_{benzazepinone}$), 136.6 (1C, C-5a $_{benzazepinone}$), 133.7 (1C, C-4 $_{benzazepinone}$), 132.8 (1C, C-9a $_{benzazepinone}$), 123.8 (1C, C-5 $_{benzazepinone}$), 121.5 (1C, C-9 $_{benzazepinone}$), 119.7 (1C, C-6 $_{benzazepinone}$), 65.1 and 65.0 (2C, CH_3O -7 $_{benzazepinone}$, CH_3O -8 $_{benzazepinone}$), 52.1 (1C, C-1 $_{benzazepinone}$). FTIR (neat): $\tilde{\nu}$ (cm^{-1}) = 3066 (C-H $_{arom}$), 2931 (C-H $_{aliph}$), 1660 (C=O), 1510 (C=C $_{arom}$).

Ethyl 5-(7,8-dimethoxy-2-oxo-1,2-dihydro-3H-benzo[d]azepin-3-yl)cyclohex-3-ene-1-carboxylate (4)

7,8-Dimethoxy-1,3-dihydro-2H-benzo[d]azepin-2-one (3, 2.44 g, 11.2 mmol, 1.3 eq) was suspended in dry tetrahydrofuran (6 mL) under N_2 atmosphere. NaH (60% suspension in paraffin oil, 446 mg, 11.15 mmol, 1.3 eq) was added and the mixture was stirred for 30 min at room temperature. The mixture was then heated to 70°C and the solvent was removed via streaming N_2 through the apparatus. After cooling to room temperature, the residue was dissolved in dry dimethyl sulfoxide (14 mL). Ethyl 5-bromocyclohex-3-ene-1-carboxylate (2b, 2.00 g, 8.58 mmol, 1 eq) was dissolved in dry dimethyl sulfoxide (3 mL) and the resulting solution was added dropwise over a period of 1 h to the reaction mixture. The mixture was stirred for 1 day at room temperature, water (15 mL) was added, and the formed precipitate was filtered off. The residue was washed with chloroform (30 mL). Additional water (20 mL) was added, the layers were separated, and the aqueous layer was extracted using chloroform (3 \times 60 mL). The combined organic layers were washed with water (2 \times 15 mL), then dried over Na_2SO_4 , filtered and the solvent was removed in vacuo. The crude product was purified via flash chromatography (cyclohexane/ethyl acetate = 2:1, \emptyset = 3 cm, h = 12 cm, V = 20 mL). The product (1.52 g) was isolated as a mixture of 86% cis-oriented and 14% trans-oriented compounds. Colorless solid, ($C_{21}H_{25}NO_5$, 371.43 g/mol, 4.10 mmol, 48%). TLC (Silica): R_f = 0.51 (cyclohexane/ethyl acetate = 2:1). mp: 117°C. Exact mass (APCI): m/z = calcd. for $C_{21}H_{25}NO_5$ [$M+H^+$] 372.1806, found 372.1810. Purity (HPLC, method Purity C): 86%, R_t = 7.7 min (cis), 14%, R_t = 7.4 min (trans). 1H NMR (400 MHz, $CDCl_3$): δ = 6.79 (s, 1H, 9- $CH_{benzazepinone}$), 6.7325 (s, 0.2H, 6- $CH_{benzazepinone}$ [trans]), 6.725 (s, 1H, 6- $CH_{benzazepinone}$ [cis]), 6.44 (d, J = 9.3 Hz, 0.2H, 5- $CH_{benzazepinone}$ [trans]), 6.39 (d, J = 9.3 Hz, 1H, 5- $CH_{benzazepinone}$ [cis]), 6.24 (d, J = 9.3 Hz, 0.2H, 4- $CH_{benzazepinone}$ [trans]), 6.20 (d, J = 9.3 Hz, 1H,

4-*CH*_{benzazepinone} [cis]), 6.14–6.04 (m, 0.2H, 3-*CH*_{cyclohexenyl} [trans]), 6.01–5.91 (m, 1H, 3-*CH*_{cyclohexenyl} [cis]), 5.61–5.54 (m, 0.2H, 4-*CH*_{cyclohexenyl} [trans]), 5.49 (d, *J* = 10.2 Hz, 1H, 4-*CH*_{cyclohexenyl} [cis]), 5.40–5.30 (m, 1H, 5-*CH*_{cyclohexenyl} [cis]), 5.27–5.20 (m, 0.2H, 3-*CH*_{cyclohexenyl} [trans]), 4.18 (q, *J* = 7.1 Hz, 0.4H, OCH₂CH₃ [trans]), 4.14–4.07 (m, 2H, OCH₂CH₃ [cis]), 3.89 (s, 4H, 8-CH₃O_{benzazepinone}), 3.88 (s, 4H, 7-CH₃O_{benzazepinone}), 3.59–3.30 (m, 3H, 2-CH₂_{benzazepinone}), 2.80–2.64 (m, 1H, 2.73, 1-CH_{cyclohexenyl}), 2.58 (m, 0.2H, 2-CHH_{cyclohexenyl} [trans]), 2.42–2.20 (m, 2.4H, 2-CH₂_{cyclohexenyl} [cis], 2-CHH_{cyclohexenyl} [trans], 6-CHH_{cyclohexenyl} [trans]), 2.20–2.10 (m, 1H, 6-CHH_{cyclohexenyl} [cis]), 1.55 (td, *J* = 12.8, 11.0 Hz, 1H, 6-CHH_{cyclohexenyl} [cis]), 1.28 (t, *J* = 7.1 Hz, 1H, OCH₂CH₃ [trans]), 1.24–1.20 (m, 3H, OCH₂CH₃ [cis]). For the ¹³C NMR spectrum, only signals of the cis-oriented derivative could be identified and assigned due to unfavorable chemical shifts and low signal intensity of the ¹³C signals of the trans-oriented derivative. ¹³C NMR (101 MHz, CDCl₃): δ = 174.5 (1C, C=O_{ester}), 167.6 (1C, C=O_{benzazepinone}), 149.9 (1C, C-8_{benzazepinone}), 148.1 (1C, C-7_{benzazepinone}), 129.9 (1C, C-3_{cyclohexenyl}), 127.8 (1C, C-4_{cyclohexenyl}), 126.5 (1C, C-5a_{benzazepinone}), 124.7 (1C, C-9a_{benzazepinone}), 124.5 (1C, C-4_{benzazepinone}), 118.0 (1C, C-5_{benzazepinone}), 111.15 (1C, C-9_{benzazepinone}), 109.6 (1C, C-6_{benzazepinone}), 60.6 (1C, OCH₂CH₃), 56.0 (2C, CH₃O-7_{benzazepinone}, CH₃O-8_{benzazepinone}), 51.4 (1C, C-5_{cyclohexenyl}), 43.4 (1C, C-1_{benzazepinone}), 39.0 (1C, C-1_{cyclohexenyl}), 30.3 (1C, C-6_{cyclohexenyl}), 27.2 (1C, C-2_{cyclohexenyl}), 14.2 (1C, OCH₂CH₃). FTIR (neat): $\tilde{\nu}$ (cm⁻¹) = 2980 (C-H_{aliph}), 1713, 1643 (C=O), 1512 (C=C_{arom}).

Ethyl 3-(7,8-dimethoxy-2-oxo-1,2,4,5-tetrahydro-3H-benzo[d]azepin-3-yl)cyclohexane-1-carboxylate (5)

Ethyl 5-(7,8-dimethoxy-2-oxo-1,2-dihydro-3H-benzo[d]azepin-3-yl)cyclohex-3-ene-1-carboxylate (**4**, 1.45 g, 3.91 mmol, 1 eq) was suspended in ethanol (60 mL) and Raney nickel suspension in water (3 mL) was added. H₂ atmosphere was applied at a pressure of 5 bar and the mixture was stirred vigorously for 5 days (after 3 days another 2 mL of Raney nickel suspension was added). The mixture was filtered through a plug of Celite, and the solvent was removed in vacuo. The crude product was purified via flash chromatography (cyclohexane/ethyl acetate = 4:6, Ø = 4.5 cm, *h* = 20 cm, *V* = 20 mL) to yield 1.35 g of a colorless oil (C₂₁H₂₅NO₅, 375.47 g/mol, 3.6 mmol, 92%) TLC (Silica): *R*_f = 0.31 (cyclohexane/ethyl acetate = 1:1 [cis]), *R*_f = 0.29 (cyclohexane/ethyl acetate = 1:1 [trans]). Exact mass (APCI): *m/z* = calcd. for C₂₁H₃₀NO₅ [M+H⁺] 376.2119, found 376.2104. Purity (HPLC, method Purity C): >99%, *R*_t = 6.20 min. ¹H NMR (400 MHz, CDCl₃): δ = 6.60 (s, 1H, 9-CH_{benzazepinone}), 6.52 (s, 1H, 6-CH_{benzazepinone}), 4.52 (tt, *J* = 12.0, 3.7 Hz, 1H, 3-CH_{cyclohexyl}), 4.11 (q, *J* = 7.1 Hz, 2H, OCH₂CH₃), 3.84 (s, 5H, 1-CH₂_{benzazepinone}, 8-CH₃O_{benzazepinone}), 3.82 (s, 3H, 7-CH₃O_{benzazepinone}), 3.72–3.67 (m, 2H, 4-CH₂_{benzazepinone}), 3.01 (dt, *J* = 5.5, 3.2 Hz, 2H, 5-CH₂_{benzazepinone}), 2.46 (tt, *J* = 12.1, 3.5 Hz, 1H, 1-CH_{cyclohexyl}), 2.33 (s, 1H, unknown impurity), 2.03–1.92 (m, 2H, 6-CHH_{cyclohexyl}, 2-CHH_{cyclohexyl}), 1.94–1.84 (m, 1H, 5-CHH_{cyclohexyl}), 1.78–1.69 (m, 1H, 4-CHH_{cyclohexyl}), 1.56 (q, *J* = 12.3 Hz, 1H, 2-CHH_{cyclohexyl}), 1.50–1.35 (m, 2H, 5-CHH_{cyclohexyl}, 4-CHH_{cyclohexyl}), 1.36–1.27

(m, 1H, 6-CHH_{cyclohexyl}), 1.24 (t, *J* = 7.1 Hz, 3H, OCH₂CH₃). ¹³C NMR (101 MHz, CDCl₃): δ = 175.2 (1C, C=O_{ester}), 172.5 (1C, C=O_{benzazepinone}), 148.1 (1C, C-7_{benzazepinone}), 147.3 (1C, C-8_{benzazepinone}), 127.2 (1C, C-5a_{benzazepinone}), 123.3 (1C, C-9a_{benzazepinone}), 114.2 (1C, C-9_{benzazepinone}), 113.3 (1C, C-6_{benzazepinone}), 60.6 (1C, OCH₂CH₃), 56.1 (2C, CH₃O-7_{benzazepinone}, CH₃O-8_{benzazepinone}), 51.5 (1C, C-3_{cyclohexyl}), 42.9 (1C, C-1_{benzazepinone}), 42.7 (1C, C-1_{cyclohexyl}), 40.5 (1C, C-4_{benzazepinone}), 34.1 (1C, C-3_{benzazepinone}), 32.9 (1C, C-2_{cyclohexyl}), 30.0 (1C, C-4_{cyclohexyl}), 28.4 (1C, C-6_{cyclohexyl}), 24.6 (1C, C-3_{cyclohexyl}), 14.3 (1C, OCH₂CH₃). FTIR (neat): $\tilde{\nu}$ (cm⁻¹) = 2933 (C-H_{aliph}), 1722, 1643 (C=O), 1517, 1422 (C=C_{arom}).

cis-3-(7,8-Dimethoxy-2-oxo-1,2,4,5-tetrahydro-3H-benzo[d]azepin-3-yl)cyclohexane-1-carboxylic acid (cis-6)

Ethyl 3-(7,8-dimethoxy-2-oxo-1,2,4,5-tetrahydro-3H-benzo[d]azepin-3-yl)cyclohexane-1-carboxylate (**5**, 1.05 g, 2.80 mmol, 1 eq) was dissolved in H₃COH (4 mL) and a solution of NaOH in H₃COH (5 M, 1 mL) was added. The mixture was stirred for 3 d at room temperature. Hydrochloric acid (2 M, 3 mL) was added, and the mixture was extracted with ethyl acetate (3 × 30 mL). The combined organic layers were dried over Na₂SO₄, filtered and the solvent was removed in vacuo to give 956 mg of colorless solid (C₁₉H₂₅NO₅, 347.41 g/mol, 2.76 mmol, 98%). TLC (Silica): *R*_f = 0.45 (CH₂Cl₂ + 8% H₃COH). mp: 116°C. Exact mass (APCI): *m/z* = calcd. for C₁₉H₂₄NO₅ [M-H⁺] 346.1660, found 346.1657. Purity (HPLC, method Purity C): 95%, *R*_t = 3.34 min. ¹H NMR (400 MHz, D₃COD): δ = 6.675 and 6.670 (s, 2H, 6-CH_{benzazepinone}, 9-CH_{benzazepinone}), 4.40 (tt, *J* = 12.1, 3.7 Hz, 1H, 3-CH_{cyclohexyl}), 3.85–3.76 (m, 10H, 1-CH₂_{benzazepinone}, 4-CH₂_{benzazepinone}, 7-CH₃O_{benzazepinone}, 8-CH₃O_{benzazepinone}), 3.03 (dd, *J* = 7.6, 4.7 Hz, 2H, 5-CH₂_{benzazepinone}), 2.43 (tt, *J* = 12.1, 3.5 Hz, 1H, 1-CH_{cyclohexyl}), 2.01–1.85 (m, 3H, 2-CHH_{cyclohexyl}, 5-CHH_{cyclohexyl}, 6-CHH_{cyclohexyl}), 1.75–1.61 (m, 2H, 2-CHH_{cyclohexyl}, 4-CHH_{cyclohexyl}), 1.61–1.24 (m, 3H, 4-CHH_{cyclohexyl}, 5-CHH_{cyclohexyl}, 6-CHH_{cyclohexyl}). ¹³C NMR (101 MHz, D₃COD): δ = 178.6 (1C, C=O_{ester}), 175.2 (1C, C=O_{benzazepinone}), 149.6 (1C, C-8_{benzazepinone}), 148.7 (1C, C-7_{benzazepinone}), 129.2 (1C, C-5a_{benzazepinone}), 124.6 (1C, C-9a_{benzazepinone}), 115.5 (1C, C-9_{benzazepinone}), 115.1 (1C, C-6_{benzazepinone}), 56.6 and 56.5 (2C, H₃CO-7_{benzazepinone}, H₃CO-8_{benzazepinone}), 53.6 (1C, C-3_{cyclohexyl}), 43.9 (1C, C-1_{cyclohexyl}), 43.2 (1C, C-5_{benzazepinone}), 41.6 (1C, C-4_{benzazepinone}), 34.5 (1C, C-5_{benzazepinone}), 33.8 (1C, C-2_{cyclohexyl}), 30.7, 29.4, and 25.7 (3C, C-4_{cyclohexyl}, C-5_{cyclohexyl}, C-6_{cyclohexyl}). FTIR (neat): $\tilde{\nu}$ (cm⁻¹) = 2980, 2970 (C-H_{aliph}), 1714, 1605 (C=O), 1519 (C=C_{arom}).

cis-3-(3-Aminocyclohexyl)-7,8-dimethoxy-1,3,4,5-tetrahydrobenzo[d]azepin-2-one (cis-7)

cis-3-(7,8-Dimethoxy-2-oxo-1,2,4,5-tetrahydro-3H-benzo[d]azepin-3-yl)cyclohexane-1-carboxylic acid (cis-6), 500 mg, 1.55 mmol, 1 eq) was dissolved in dry toluene (8 mL) under N₂ atmosphere. Dry triethylamine (240 µL, 1.73 mmol, 1.2 eq) and diphenylphosphoryl azide (400 µL, 1.58 mmol, 1.1 eq) were added, and the mixture was heated to 90°C for 2.5 h. Tetrahydrofuran (15 mL) was added and the mixture was cooled to 5°C. Hydrochloric acid (2 M, 5 mL) was added and the mixture was stirred overnight while being allowed to warm up to room temperature. Additional hydrochloric acid (1 M, 20 mL) was added, and the mixture

was washed with diethyl ether (2 × 40 mL). The aqueous layer was basified using NaOH (2.5 M) to pH = 11 and was extracted with CH₂Cl₂ (4 × 50 mL). The combined organic layers were dried over Na₂SO₄, filtered and the solvent was removed in vacuo. The crude product was purified via flash chromatography (CH₂Cl₂ + 10% H₃COH + 1% NH₄OH, Ø = 3 cm, h = 16 cm, V = 20 mL) to yield 290 mg of a colorless oil (C₁₈H₂₆N₂O₃, 318.42 g/mol, 0.91 mmol, 63%). TLC (Silica): R_f = 0.35 (CH₂Cl₂ + 10% H₃COH + 1% NH₄OH). Exact mass (APCI): m/z = calcd. for C₁₈H₂₇N₂O₃ [M+H]⁺ 319.2016, found 319.2005. ¹H NMR (400 MHz, CDCl₃): δ = 6.59 (s, 1H, 9-CH₂benzazepinone), 6.52 (s, 1H, 6-CH₂benzazepinone), 4.50 (tt, J = 12.1, 3.6 Hz, 1H, 3-CH₂cyclohexyl), 3.83 (s, 3H, 8-CH₃O_{benzazepinone}), 3.82–3.80 (m, 5H, 7-CH₃O_{benzazepinone}, 1-CH₂benzazepinone), 3.74–3.60 (m, 2H, 4-CH₂benzazepinone), 3.01 (dd, J = 7.6, 4.7 Hz, 2H, 5-CH₂benzazepinone), 2.89 (tt, J = 11.2, 3.9 Hz, 1H, 1-CH₂cyclohexyl), 2.18 (s, 2H, NH), 1.97–1.76 (m, 3H, 2-CHH_{cyclohexyl}, 5-CHH_{cyclohexyl}, 6-CHH_{cyclohexyl}), 1.74–1.64 (m, 1H, 4-CHH_{cyclohexyl}), 1.49–1.22 (m, 3H, 2-CHH_{cyclohexyl}, 4-CHH_{cyclohexyl}, 5-CHH_{cyclohexyl}), 1.12–0.98 (m, 1H, 6-CHH_{cyclohexyl}). ¹³C NMR (101 MHz, CDCl₃): δ = 172.3 (1C, C=O_{benzazepinone}), 148.0 (1C, C-8_{benzazepinone}), 147.3 (1C, C-7_{benzazepinone}), 127.3 (1C, C-5a_{benzazepinone}), 123.5 (1C, C-9a_{benzazepinone}), 114.2 (1C, C-9_{benzazepinone}), 113.3 (1C, C-6_{benzazepinone}), 56.1 (2C, CH₃OC-7_{benzazepinone}, CH₃OC-8_{benzazepinone}), 51.0 (1C, C-3_{cyclohexyl}), 49.8 (1C, C-1_{cyclohexyl}), 43.2 (1C, C-1_{benzazepinone}), 40.5 (1C, C-4_{benzazepinone}), 40.4 (1C, C-2_{cyclohexyl}), 34.9 (1C, C-6_{cyclohexyl}), 34.1 (1C, C-5_{benzazepinone}), 29.7 (1C, C-4_{cyclohexyl}), 23.3 (1C, C-5_{cyclohexyl}). FTIR (neat): ν̄ (cm⁻¹) = 2980, 2928 (N-H, C-H_{aliph}), 1608 (C=O), 1518 (C=C_{arom}).

4.2 | Biological assays

4.2.1 | Animals

To characterize the native I_h current of thalamocortical (TC) neurons in the ventrobasal complex (VB) of the thalamus and the activity-dependent effect of EC18, we performed electrophysiological experiments in C57BL/6J mice of both genders (n = 16). Mice were purchased from ENVIGO (Germany) and housed in groups of five individuals at the Institute of Physiology I (Westfälische Wilhelms-Universität) with at least 1 week of habituation period, before the start of experiments. Animals were killed at the age of 4–6 weeks. All experimental procedures were performed in accordance with the principles approved by local authorities (review board institution: Landesamt für Natur, Umwelt und Verbraucherschutz Nordrhein-Westfalen, LANUV NRW). Efforts were made to minimize the number and degree of discomfort to animals used in the present study.

4.2.2 | Preparation of acute brain slices for whole-cell patch clamp recordings

Animals were killed according to effective legal standards without anesthesia using DecapiCones (Braintree Scientific Inc.), and

brain tissue was rapidly removed from the skull. Brain slices (250 μm) were prepared as coronal sections in ice-cold oxygenated slicing solution, containing (in mM): sucrose, 200; PIPES, 20; KCl, 2.5; NaH₂PO₄, 1.25; MgSO₄, 10; CaCl₂, 0.5; dextrose, 10; pH 7.35. Before electrophysiological recordings, slices were transferred and kept first in a chamber with artificial cerebrospinal fluid (aCSF; containing in mM: NaCl, 120; KCl, 2.5; NaH₂PO₄, 1.25; NaHCO₃, 22; MgSO₄, 2; CaCl₂, 2; glucose, 25; pH 7.35) at 32°C for 20 min and thereafter at the room temperature (RT). The incubation solution was continuously bubbled with carbogen. EC18 was directly added to the aCSF, resulting in a final concentration between 0.1 and 100 μM.

4.2.3 | Whole-cell voltage-clamp recordings in acute brain slices

Whole-cell voltage-clamp recordings of TC VB neurons were carried out in external standard aCSF solution containing (in mM) NaCl, 125; KCl, 2.5; NaH₂PO₄, 1.25; NaHCO₃, 1.25; MgSO₄, 2; CaCl₂, 2; Glucose, 10; BaCl₂, 0.5; pH 7.25 (adjusted and maintained with continuous bubbling with carbogen) at 32 ± 1°C. Patch pipettes were pulled from borosilicate glass (GC150T-10; Clark Electromedical Instruments) and had a resistance of 2.8–3.5 MΩ. The internal pipette solution contained the following (in mM): K-gluconate, 88; K₃-citrate, 20; NaCl, 10; HEPES, 10; MgCl₂, 1; CaCl₂, 0.5; BAPTA, 3; Mg-ATP, 3; Na₂-GTP, 0.5. The internal solution was set to a pH of 7.35 with KOH and an osmolarity of 295 mOsmol/kg. All recordings were performed on the soma of TC neurons using an EPC-10 amplifier (HEKA Elektronik). The access resistance was in the range of 5–25 MΩ and was monitored throughout the whole experiment. Cells with access resistance of more than 25 MΩ were discarded from the experiments. Voltage-clamp experiments were controlled by the software PatchMaster (HEKA Elektronik), operating on an IBM-compatible personal computer. Measurements were corrected for a liquid junction of 10 mV.

The voltage protocols which we used to examine the native I_h current of TC VB neurons were designed to increase the stability of whole-cell recordings and account for increasingly fast activation kinetics of the current. I_h current was activated by families of hyperpolarizing steps (–40 to –130 mV) of –10 mV increments from a holding potential of –40 mV. The length of each sweep was 18 s, split into varying segments for the holding potential and the hyperpolarizing pulse as well as a fixed 1 s pulse to –100 mV to obtain deactivating tail currents. With increasing hyperpolarization, the pulse length was shortened by 1.5 s resulting in a 3 s pulse length at the –130 mV step (Figure 7a). Steady-state activation of I_h current was assessed under control conditions and following 20 min wash-in of EC18 (30 μM) using two experimental paradigms. In one set of experiments (Set I), no I_h current activation occurred between the families of hyperpolarizing steps. In another set of experiments (Set II), a single pulse to –110 mV was given every 60 s during the 20 min wash in period of EC18 (30 μM; Figure 7b). Thus, TC neurons were

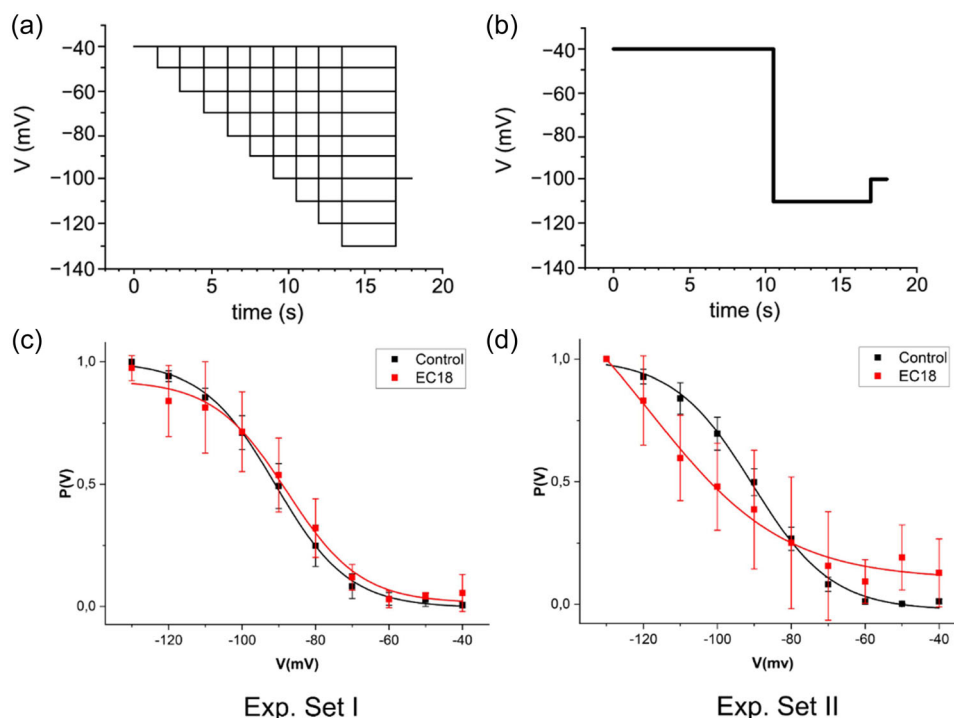


FIGURE 7 Use-dependency of the steady-state activation curve of I_h current. (a) Pulse protocol used to determine the I_h current activation curve in acute brain slices under control conditions and in the presence of EC18. (b) Pulse protocol used for repetitive activation of I_h current during EC18 application in one set of experiments (Set II). (c, d) Steady-state activation curves before (in black) and after application of 30 μ M EC18 (in red) without (C; Set I) and with (D; Set II) repetitive activation of I_h current.

stimulated by in total of 20 sweeps before a complete family of steps was elicited in the presence of EC18.

To determine the dosage-dependent inhibition of I_h current in TC VB neurons by EC18, we performed the whole-cell recordings using maximal hyperpolarizing steps from -40 to -110 mV with other parameters of the recording protocol (pulse length, sweep duration) unchanged. The duration of the EC18 application was set to 15 min, considering that during Exp. Set II, the compound already displayed significant changes in the properties of I_h current at this time point.

Steady-state activation of I_h , indicating the fraction of HCN channel opening $p(V)$, was estimated by normalizing the mean tail current amplitudes (I) 150–250 ms after stepping to a constant potential of -100 mV from variable step amplitudes (from -40 to -130 mV) using the following equation:

$$p(V) = \frac{I - I_{\min}}{I_{\max} - I_{\min}},$$

where I_{\max} is the tail current amplitude for the voltage step from -130 to -100 mV and I_{\min} represents the voltage step from -40 to -100 mV, respectively. I_h activation was fitted by a Boltzmann equation of the following form:

$$p(V) = \left(1 + e^{\frac{V - V_{0.5}}{k}}\right)^{-1},$$

where, k represents the slope factor. The amplitude of I_h was calculated by subtracting the instantaneous current amplitude from

the steady-state current. The density of I_h (current density, CD) was calculated by dividing the maximum I_h current amplitude at -130 mV by the membrane capacitance obtained during whole-cell recordings. To analyze CD during repetitive activation of HCN channels during EC18 application (Set II), I_h current amplitude at -110 mV was divided by the membrane capacitance of cells. The time course of I_h in TC VB neurons (two components of HCN channel activation—fast and slow) was calculated by fitting the hyperpolarizing pulse step to -130 mV with a dual exponential equation:

$$I_h(t) = A_0 + A_1 e^{(-t/\tau_1)} + A_2 e^{(-t/\tau_2)},$$

where, $I_h(t)$ is the total amplitude of the current at time t , and A_1 and A_2 are the respective amplitudes of the components with fast (τ_1) and slow (τ_2) time constants.

4.2.4 | Data analysis and statistics

For data assembling and analyses, Excel (Microsoft), OriginPro 2020/21 (OriginLab Corporation), and GraphPad Prism 7.01 (GraphPad Software) were used. Comparison of I_h current characteristics with and without EC18 was performed by using one-way analysis of variance (ANOVA) (post hoc mean comparison using Tukey Test). Comparison of EC18 recordings between the two experimental sets and during repetitive activation of HCN channels in Set II was

performed by two-way ANOVA (post hoc mean comparison Tukey test, based on two main variables: application of EC18 and the repetitive current activation during compound application). All the calculated results are presented as mean \pm SEM. The significance of statistical difference was noted as * if $p < 0.05$, ** if $p < 0.01$, *** if $p < 0.001$, and as **** if $p < 0.0001$.

4.2.5 | Splenocyte isolation

Splenocytes were isolated from C57BL/6J mice as described before.^[18] Erythrocyte lysis was performed in ACK buffer (ddH₂O with 0.15 M NH₄Cl, 10 mM KHCO₃ and 0.1 mM EDTA, pH of 7.3) for 1 min. Afterward, cells were washed and seeded in splenocyte medium (DMEM containing 10 mM HEPES, 5% fetal bovine serum, 25 μ g/mL gentamycin, 50 μ M 2-mercaptoethanol, 1% nonessential amino acids) at a final concentration of 3×10^6 cells/well in flat bottom 24 well plates. For splenocyte stimulation, plates were pre-coated with purified anti-CD3 (2 μ g/mL; clone:145-2C11; Biolegend) overnight at 4°C. After seeding, purified anti-CD28 (1 μ g/mL; Biolegend) was added for optimal stimulation. The stimulated groups were either treated with vehicle or with EC18 (0.1, 1, 5, 10 μ M). Thereafter splenocytes were incubated for 2 days in a humidified incubator with 5% CO₂ at 37°C.

4.2.6 | Flow cytometry

After 2 days in vitro splenocytes were collected and analyzed by flow cytometry. Therefore, cells were stained in FACS buffer (1x PBS containing 5% FCS, 0.4% EDTA) with the following antibodies: Anti-mouse-CD3 Brilliant Violet 510™ (clone: 17A2, Biolegend); anti-mouse-CD4 FITC (clone: H129.19, Biolegend), anti-mouse-CD8a PE (clone: 53-6.7, Biolegend), anti-mouse-CD25 PE/Cy7 (clone: PC61, Biolegend), anti-Maus-CD69 eFluor 450 (clone: H1.2F3, Thermo Fisher Scientific). Living splenocytes were selected using the FVD780 dye in the side and forward scatter. Measurements were performed on a Gallios flow cytometer (Beckmann Coulter GmbH) and data were analyzed using Kaluza software 2.1 (Beckman Coulter).

4.2.7 | Cell culture

hiPSC culture

Human iPS cells (hiPSC; SFS.1) were incubated at 37°C/5% CO₂. The hiPSC were cultured in the cell culture medium FTDA-medium consisting of (DMEM/F12) (Invitrogen #21331020), 5 μ g/mL ITS (Becton Dickinson #354350), 0.1% human serum albumin (Biological Industries #05-720-1B), 1X CD Lipid Concentrate (Invitrogen #1905031), 1X Penicillin/Streptomycin/Glutamine (Life Technologies #10378016), 10 ng/mL FGF2 (PeproTech #100-18B), 5 ng/mL Activin A (eBioscience #34-8993-85), 0.4 μ g/mL TGF β 1 (eBioscience #34-8348-82), and 50 nM Dorsomorphin (Santa Cruz #sc-200689)

ensuring the preservation of pluripotency.^[19,20] The medium was exchanged daily. After 4 days of culture, when cells reached 100% confluence, passaging was performed by PBS washing and subsequent Accutase® solution (Sigma #A6964) incubation in addition to 10 μ M Y-27632 (AbcamBiochemicals # ab120129) for 10 min at 37°C until complete cell detachment. FTDA medium with 10 μ M Y-27632 was added to stop the Accutase® reaction. The cell suspension was centrifuged for 2 min at 200 \times g and resuspended in FTDA medium with 10 μ M Y-27632. For maintenance culture, 600,000 cells were reseeded into 6-well plates coated with 1:75 diluted Matrigel® (Becton Dickinson #354263). The next day, medium change was performed with FTDA without Y-27632.

Differentiation of SFS.1-hiPSC into HCN4-positive cardiomyocytes

SFS.1 hiPSC were detached with Accutase® for 10 min and treated as previously described. After centrifugation for 2 min at 200 \times g, day zero differentiation medium consisting of KO-DMEM (Life Technologies #10829018), 1 \times Penicillin/Streptomycin/Glutamine, 5 μ g/mL ITS, 10 μ M Y-27632, 20 ng/mL FGF2, 1 nM CHIR-99021 (Axon Medchem #Axon1386), and 0.25 to 2.0 nM BMP-4 (R&D # 314-BP-010) was used to resuspend the cells. The concentration of BMP-4 was tested regularly to ensure optimal differentiation. The cells were seeded on Matrigel® coated 24 wells at 550,000 cells/well. Medium change was performed the next day. Thereby, the day zero medium was changed to TS-ASC medium consisting of (KO-DMEM, 5.5 mg/L Transferrin (Sigma #T8158-100MG), 6.75 μ g/L Selenium (Sigma # S5261-10G), 1X Penicillin/Streptomycin/Glutamine, 250 μ M ascorbate (Sigma # 49752-10G). The cultivation of the cells with TS-ASC medium lasted for exactly 24 h. Then, the medium was changed to TS-ASC + 0.5 mM C59 (Tocris #5148). The cells were kept in TS-ASC + C59 for another 48 h with a medium exchange after 24 h. Afterward, the cells were kept in TS-ASC medium for another 5 days until spontaneous beating was observed.^[21] The cells were washed with PBS and treated with TrypLE Select (10 \times) (Life Technologies # 12563011) supplemented with 10 μ M Y-27632 for 15 min at 37°C. After centrifugation for 3 min at 200 \times g, cells were resuspended in KO-THAI medium (KO-DMEM, 1 \times Penicillin/Streptomycin/Glutamine, 0.2% human serum albumin, 250 μ M ascorbate, 5 μ g/mL ITS, and 0.004% (v/v) Thioglycerol + 10 μ M Y-27632) and seeded at a 1:6 ratio on 24-wells, coated with 1:75 diluted Matrigel® and 0.2% gelatin. After 24 h, the medium was changed to KO-THAI medium without Y-27632. For HCN4 expression elevation, the KO-THAI medium was changed to a maturation medium after 24 h. The maturation medium consisted of KO-DMEM, 20% FBS superior (Sigma Aldrich #S0615), and 1 mM CaCl₂, which is an adaptation of the maturation medium by Schweizer et al.^[22] The hiPSC-derived cardiomyocytes were cultivated in a maturation medium for another 4 weeks until reaching adequate maturity as described by Peischard et al.^[11]

4.2.8 | Immunostaining

Thirty-five days differentiated HCN4-expressing hiPSC-derived cardiomyocytes were seeded on 12 mm glass coverslips previously coated with

0.2% gelatine for 1 h and additional FBS for 15 min. The cells were cultivated at 37°C and 5% CO₂ overnight. After 24 h, cell fixation was performed with 3.7% PFA/PBS for 15 min. Afterward, the fixed cells were washed with PBS twice for 5 min. Blocking was done with 2% BSA, and 2% glycine with added 0.2% Triton-X in PBS-Tween (PBS-T) for 1 h. After washing with PBS-T twice, the cells were rinsed and incubated with the primary antibodies against N-Cadherin (ab22744; Abcam), HCN4 (APC-052; Alomone Labs) at 4°C, overnight in 0.5% BSA, PBS-T at a ratio of 1:400. The next day, the cells were washed with PBS-T three times for 5 min and incubated with the secondary antibodies (115-585-044; Jackson Immuno Research, SAB4600036; Sigma Aldrich or A-11046; Thermo Fisher) in 0.5% BSA, PBS-T in a ratio of 1:1000. The stained cells were fixed on glass with Aquapoly-mount® (18606; Polysciences) and imaged with a DMI4000 confocal microscope (Leica) equipped with a 63x oil immersion objective.

4.2.9 | Contraction analysis

Spontaneous beating hiPSC-derived cardiomyocytes were seeded into 1:75 diluted Matrigel® and 0.2% gelatin-coated 24 well plates and cultured for 48 h in a maturation medium. After 48 h a medium change was done and the cells were cultivated for another 24 h at 37°C and 5% CO₂. The cells were then imaged at 30 Hz and 10× magnification under basal conditions, under β -adrenergic stimulation with 1 μ M isoprenaline, and after subsequent EC18 application at a concentration of 100 μ M.^[10] The contractions were counted and statistically analyzed. Significance between groups was tested with paired *t*-test. Contraction profiling was performed with the muscle motion plugin for ImageJ Fiji.

4.2.10 | P2X receptor assays

The P2XR assays were performed as previously described by Isaak et al.^[23]

ACKNOWLEDGMENTS

Anna Junker thanks the German Research Foundation (DFG) for the financial support (JU 2966/2-1). Anna Junker, Petra Hundehege, Guiscard Seeböhm, and Thomas Budde thank the German Research Foundation (DFG) for the financial support (GRK2515/1-1, BU1019/16-1). SGM thanks the German Research Foundation (DFG) for the financial support (INST 2105/27-1 FUGG).

CONFLICTS OF INTEREST STATEMENT

The authors declare no conflicts of interest.

ORCID

Anna Junker  <http://orcid.org/0000-0001-5151-0930>

REFERENCES

- [1] J. Stieber, S. Herrmann, S. Feil, J. Löster, R. Feil, M. Biel, F. Hofmann, A. Ludwig, *Proc. Natl. Acad. Sci. USA* **2003**, *100*, 15235.
- [2] M. Zobeiri, R. Chaudhary, A. Blaich, M. Rottmann, S. Herrmann, P. Meuth, P. Bista, T. Kanyshkova, A. Lüttjohann, V. Narayanan, P. Hundehege, S. G. Meuth, M. N. Romanelli, F. J. Urbano, H. C. Pape, T. Budde, A. Ludwig, *Cereb. Cortex* **2019**, *29*, 2291.
- [3] M. Zobeiri, G. van Luijtelaar, T. Budde, I. V. Sysoev, *Brain Connect.* **2019**, *9*, 273.
- [4] T. Kanyshkova, M. Pawlowski, P. Meuth, C. Dube, R. A. Bender, A. L. Brewster, A. Baumann, T. Z. Baram, H. C. Pape, T. Budde, *J. Neurosci.* **2009**, *29*, 8847.
- [5] T. Kanyshkova, P. Meuth, P. Bista, Z. Liu, P. Ehling, L. Caputi, M. Doengi, D. M. Chetkovich, H. C. Pape, T. Budde, *Neurobiol. Dis.* **2012**, *45*, 450.
- [6] Q. Kharouf, A. M. Phillips, L. E. Bleakley, E. Morrisroe, J. Oyrer, L. Jia, A. Ludwig, L. Jin, J. A. Nicolazzo, E. Cerbai, M. N. Romanelli, S. Petrou, C. A. Reid, *Br. J. Pharmacol.* **2020**, *177*, 3712.
- [7] U. Chaudhary, I. Vlachos, J. B. Zimmermann, A. Espinosa, A. Tonin, A. Jaramillo-Gonzalez, M. Khalili-Ardali, H. Topka, J. Lehmberg, G. M. Friehs, A. Woodtli, J. P. Donoghue, N. Birbaumer, *Nat. Commun.* **2022**, *13*, 1236.
- [8] T. Oniani, L. Vinnenberg, R. Chaudhary, J. A. Schreiber, K. Riske, B. Williams, H.-C. Pape, J. A. White, A. Junker, G. Seeböhm, S. G. Meuth, P. Hundehege, T. Budde, M. Zobeiri, *Int. J. Mol. Sci.* **2022**, *23*, 6285.
- [9] Y. Iacone, T. P. Morais, F. David, F. Delicata, J. Sandle, T. Raffai, H. R. Parri, J. J. Weisser, C. Bundgaard, I. V. Klewe, G. Tamás, M. S. Thomsen, V. Crunelli, M. L. Lörincz, *Epilepsia* **2021**, *62*, 1729.
- [10] M. N. Romanelli, M. Del Lungo, L. Guandalini, M. Zobeiri, A. Gyökeres, T. Árpádfy-Lovas, I. Koncz, L. Sartiani, G. Bartolucci, S. Dei, D. Manetti, E. Teodori, T. Budde, E. Cerbai, *ACS Med. Chem. Lett.* **2019**, *10*, 584.
- [11] S. Peischard, M. Möller, P. Disse, H. T. Ho, A. O. Verkerk, N. Strutz-Seeböhm, T. Budde, S. G. Meuth, P. A. Schweizer, S. Morris, L. Mücher, V. Eisner, D. Thomas, K. Klingel, K. Busch, G. Seeböhm, *Cell. Mol. Life Sci.* **2022**, *79*, 440.
- [12] M. Reiffen, W. Eberlein, P. Mueller, M. Psiorz, K. Noll, J. Heider, C. Lillie, W. Kobinger, P. Luger, *J. Med. Chem.* **1990**, *33*, 1496.
- [13] A. Ludwig, *EMBO J.* **2003**, *22*, 216.
- [14] M. Del Lungo, M. Melchiorre, L. Guandalini, L. Sartiani, A. Mugelli, I. Koncz, T. Szel, A. Varro, M. N. Romanelli, E. Cerbai, *Br. J. Pharmacol.* **2012**, *166*, 602.
- [15] R. Rahmzadeh, W. Brück, A. Minagar, M. A. Sahraian, *Rev. Neurosci.* **2018**, *30*, 67.
- [16] A. Caruso, S. Licenziati, M. Corulli, A. D. Canaris, M. A. De Francesco, S. Fiorentini, L. Peroni, F. Fallacara, F. Dima, A. Balsari, A. Turano, *Cytometry* **1997**, *27*, 71.
- [17] K. Radulovic, J. H. Niess, *J. Immunol. Res.* **2015**, *2015*, 497056.
- [18] P. Hundehege, J. Fernandez-Orth, P. Römer, T. Ruck, T. Muntefering, S. Eichler, M. Cerina, L. Epping, S. Albrecht, A. F. Menke, K. Birkner, K. Göbel, T. Budde, F. Zipp, H. Wiendl, A. Gorji, S. Bittner, S. G. Meuth, *Neurosignals* **2018**, *26*, 77.
- [19] S. Peischard, I. Piccini, N. Strutz-Seeböhm, B. Greber, G. Seeböhm, *Pflügers Archiv Eur. J. Physiol.* **2017**, *469*, 1233.
- [20] S. Frank, M. Zhang, H. R. Schöler, B. Greber, *PLoS One* **2012**, *7*, e41958.
- [21] S. Peischard, H. T. Ho, I. Piccini, N. Strutz-Seeböhm, A. Röpke, I. Liashkovich, H. Gosain, B. Rieger, K. Klingel, B. Eggers, K. Marcus, W. A. Linke, F. U. Müller, S. Ludwig, B. Greber, K. Busch, G. Seeböhm, *Sci. Rep.* **2020**, *10*, 16804.
- [22] P. A. Schweizer, F. F. Darche, N. D. Ullrich, P. Geschwill, B. Greber, R. Rivinius, C. Seyler, K. Müller-Decker, A. Draguhn, J. Utikal,

M. Koenen, H. A. Katus, D. Thomas, *Stem Cell Res. Ther.* **2017**, *8*, 229.

- [23] A. Isaak, C. Dobelmann, F. T. Füsser, K. S. Erlitz, O. Koch, A. Junker, *J. Med. Chem.* **2022**, *65*, 11291.

SUPPORTING INFORMATION

Additional supporting information can be found online in the Supporting Information section at the end of this article.

How to cite this article: M. Patberg, T. Oniani, P. Disse, S. Peischard, L. Vinnenberg, M. Zobeiri, M. N. Romanelli, L. Epping, H. Wiendl, S. G. Meuth, P. Hundede, G. Seebohm, T. Budde, A. Junker, *Arch. Pharm.* **2023**, e2200665.
<https://doi.org/10.1002/ardp.202200665>